

<b>REPORT DOCUMENTATION PAGE</b>			Form Approved OMB NO. 0704-0188	
Public Reporting burden for this collection of information is estimated to average 1 hour per response, including the time for reviewing instructions, searching existing data sources, gathering and maintaining the data needed, and completing and reviewing the collection of information. Send comment regarding this burden estimate or any other aspect of this collection of information, including suggestions for reducing this burden, to Washington Headquarters Services, Directorate for Information Operations and Reports, 1215 Jefferson Davis Highway, Suite 1204, Arlington, VA 22202-4302, and to the Office of Management and Budget, Paperwork Reduction Project (0704-0188,) Washington, DC 20503.				
1. AGENCY USE ONLY (Leave Blank)		2. REPORT DATE September 30, 1998		3. REPORT TYPE AND DATES COVERED Final Report; July 1, 1992 - June 30, 1998
4. TITLE AND SUBTITLE Ignition, Combustion and Kinetics of Energetic Materials		5. FUNDING NUMBERS DAAL03-92-G-0118		
6. AUTHOR(S) K.K. Kuo, S. T. Thynell, T.B. Brill, V. Yang, T.A. Litzinger, and P.W. Brown				
7. PERFORMING ORGANIZATION NAME(S) AND ADDRESS(ES) Department of Mechanical and Nuclear Engineering The Pennsylvania State University University Park, PA 16802		8. PERFORMING ORGANIZATION REPORT NUMBER  NONE		
9. SPONSORING / MONITORING AGENCY NAME(S) AND ADDRESS(ES) U. S. Army Research Office P.O. Box 12211 Research Triangle Park, NC 27709-2211		10. SPONSORING / MONITORING AGENCY REPORT NUMBER  ARO 30344.17-C H-U R 1		
11. SUPPLEMENTARY NOTES The views, opinions and/or findings contained in this report are those of the author(s) and should not be construed as an official Department of the Army position, policy or decision, unless so designated by the documentation.				
12 a. DISTRIBUTION / AVAILABILITY STATEMENT Approved for public release; distribution unlimited.		12 b. DISTRIBUTION CODE		
13. ABSTRACT (Maximum 200 words) To develop a comprehensive model of nitramine propellant ignition and combustion, the appropriate numerical analysis was developed to solve both transient and steady-state combustion, including detailed finite-rate chemical kinetics, thermodynamic phase transition, and sub-surface reactions. The model was advanced to predict ignition phenomena. Modeling work was complemented by conducting various experiments. Using fast thermolysis, significant accomplishments were made in studies of the decomposition behavior of propellant ingredients, such as RDX, cellulose acetate butyrate, nitrocellulose, and mixtures of RDX and binders. Intrusive mass spectroscopic techniques were utilized to acquire gas-phase species profiles under laser-assisted burning of monopropellants and composite propellants. Nonintrusive diagnostic techniques were developed and used to determine temperature and species profiles within propellant flames at elevated pressures, which are needed for model validation. Temperature sensitivities were deduced for RDX and nitramine propellants, and ignition delays were deduced for RDX, HMX and RDX/CAB pseudo-propellants. In situ observation of burning surfaces revealed the formation of complex, sooty-like structures and intermittent flame attachment. A liquid strand burner was established and successfully demonstrated to have the capability of maintaining a steady liquid propellant (LP) burning surface at the tip of the feeding tube using nitromethane. The burning behavior of nitromethane was also characterized.				
14. SUBJECT TERMS RDX monopropellant, two-phase subsurface reaction, detailed chemical kinetics, ignition, steady-state combustion, thermal decomposition, binder ingredients, laser pyrolysis, temperature and species profiling, phase relationships, FTIR and UV/visible absorption spectroscopy, mass spectroscopy, nitromethane, pseudo-propellants			15. NUMBER OF PAGES 45	
			16. PRICE CODE	
17. SECURITY CLASSIFICATION OR REPORT UNCLASSIFIED	18. SECURITY CLASSIFICATION ON THIS PAGE UNCLASSIFIED	19. SECURITY CLASSIFICATION OF ABSTRACT UNCLASSIFIED	20. LIMITATION OF ABSTRACT UL	

NSN 7540-01-280-5500

Standard Form 298 (Rev.2-89)  
Prescribed by ANSI Std. Z39-18  
298-102

19981222 071

## TABLE OF CONTENTS

TABLE OF CONTENTS .....	2
LIST OF FIGURES .....	4
LIST OF TABLES.....	5
A. OVERALL STATEMENT OF PROBLEM.....	6
B. SUMMARY OF THE MOST IMPORTANT RESULTS .....	6
I. Numerical Simulation of Propellant Combustion with Detailed Chemical Kinetics .....	6
I.1 Statement of Problem.....	6
I.2 Summary of Most Important Results .....	6
I.3 References.....	10
II. Micro-probe Mass Spectrometer Studies of Propellant Flames.....	11
II.1 Statement of Problem.....	11
II.2 Summary of Most Important Results .....	11
II.3 References .....	15
III. FTIR Absorption Spectrometry of Propellant Flames.....	15
III.1 Statement of Problem .....	15
III.2 Summary of Most Important Results.....	16
III.3 References.....	19
IV. Ignition Delay, Temperature Sensitivity, and UV/Visible Absorption Spectroscopy Measurements of Solid Propellants.....	20
IV.1 Statement of Problem.....	20
IV.2 Summary of Most Important Results .....	20
IV.3 References .....	29
V. Thermal Decomposition Studies of Nitramine Propellant Binder Ingredients .....	30
V.1 Statement of Problem .....	30
V.2 Summary of Most Important Results .....	30
V.3 References.....	31
VI. In Situ Observation of Burning Surface Phenomena.....	32
VI.1 Statement of Problem.....	32
VI.2 Summary of Most Important Results .....	32
VI.3 References .....	34
VII. Reactions of RDX and Nitramine-based Propellants.....	34
VII.1 Statement of Problem.....	34
VII.2 Summary of Most Important Results.....	34
VII.3 References .....	35
VIII. Condensed-phase Interactions between RDX and Common Solid Propellant Binders..	35
VIII.1 Statement of Problem .....	35
VIII.2 Summary of Most Important Results.....	35
VIII.3 References.....	36
IX. Effects of Processing Procedures on Pseudo-Propellant Flame Structure .....	36
IX.1 Statement of Problem.....	36
IX.2 Summary of Most Important Results .....	36
IX.3 References .....	36

X. Nitromethane Combustion .....	37
X.1 Statement of Problem .....	37
X.2 Summary of Most Important Results .....	37
X.3 References.....	38
C. LIST OF PUBLICATIONS AND TECHNICAL REPORTS.....	38
D. LIST OF PARTICIPATING SCIENTIFIC PERSONNEL AND DEGREES	
RECEIVED .....	44
I. Personnel.....	44
II. Degrees Awarded.....	44
E. INVENTIONS .....	45

## LIST OF FIGURES

Figure 1.1 Distributions of temperature and major species concentrations of self-sustained RDX combustion at 1 atm. ....	7
Figure 1.2 Close-up view of temperature and species-concentration profiles in subsurface region for self-sustained RDX combustion at 1 atm. ....	8
Figure 1.3 Temperature, void fraction, and species-concentration profiles in condensed phase for RDX/GAP pseudo-propellant combustion. ....	9
Figure 1.4 Temperature and species-concentration profiles in gas phase for RDX/GAP pseudo-propellant combustion. ....	10
Figure 1.5 Predicted temperature profiles at various times for laser-induced ignition of RDX monopropellant at 1 atm. ....	10
Figure 2.1 Comparison of $\text{NO}_2$ and $\text{N}_2\text{O}$ profiles for RDX and RDX/CAB at 1 atm and $400\text{W}/\text{cm}^2$ in argon. ....	12
Figure 2.2 Temperature profiles for RDX, RDX/CAB, XM39 and M43 at 1 atm and $400\text{W}/\text{cm}^2$ in argon. ....	13
Figure 2.3 Comparison of $\text{NO}_2$ , $\text{N}_2\text{O}$ profiles for XM39 and M43 at 1 atm and $100\text{W}/\text{cm}^2$ in argon. ....	13
Figure 2.4 Comparison of CO, NO and temperature profiles for XM39 at 1 atm and $100\text{W}/\text{cm}^2$ in argon and air. ....	14
Figure 3.1 Schematic diagram of the FTIR beam propagation through the solid-propellant flame. ....	16
Figure 3.2 Temperature profiles of an XM39 propellant flame at 15 atm using FTIR spectroscopy and Pt/Pt-10 % Rh (S-type) thermocouple. ....	17
Figure 3.3 Temperature profiles of an XM39 propellant flame at 22 atm using FTIR spectroscopy and Pt/Pt-10 % Rh (S-type) thermocouple. ....	18
Figure 3.4 Deduced CO and NO mole-fraction profiles of an XM39 flame at 15 atm. ....	19
Figure 4.1 Temperature and NO concentration profiles for M43 propellant at 1.6MPa. ....	23
Figure 4.2 Deduced gas-phase temperature and OH mole fraction profiles of RDX flame at 0.45 MPa. ....	24
Figure 4.3 Deduced gas-phase temperature and OH mole fraction profiles of RDX/CAB (86/14%) flame at 0.45 MPa. ....	25
Figure 4.4 Burning rates of pure RDX as a function of pressure and initial temperature. ....	26
Figure 4.5 Ignition delay times for pure RDX. ....	27
Figure 4.6 Ignition delay times for pure HMX. ....	27
Figure 4.7 Ignition delay times for RDX/CAB (86/14%) pseudo propellant. ....	28
Figure 6.1 Thick foam layer on burning surface of RDX at 0.17 MPa (10 psig). ....	33
Figure 6.2 Flame attachment to agglomerates on M43 at 1.23 MPa (165 psig). ....	33
Figure 6.3 Flame attachment to carbonaceous flakes on JA-2 at 1.48 MPa (200 psig). ....	34
Figure 10.1 Burning rate of nitromethane at different pressures and initial temperatures. ....	37

## **LIST OF TABLES**

Table 2.1	Burn rate and surface temperature data for various propellants at 1 atm in argon.....	15
Table 4.1	Flame temperatures and OH concentration of JA-2 propellant at different pressures.	22

## A. OVERALL STATEMENT OF PROBLEM

The final progress report of this project, focused on the ignition and combustion behavior of solid propellants, is summarized in ten different categories, including: (1) numerical simulation of propellant combustion with detailed chemical kinetics, (2) microprobe/mass spectrometer studies of propellant flames, (3) FTIR absorption spectrometry of propellant flames, (4) ignition delay, temperature sensitivity, and UV/Visible absorption spectroscopy measurements of solid propellants, (5) thermal decomposition studies of nitramine propellant binder ingredients, (6) in situ observation of burning surface phenomena, (7) reactions of RDX and nitramine-based propellants, (8) condensed-phase interactions between RDX and common solid propellant binders, (9) effects of processing procedures on pseudo-propellant flame structure, and (10) nitromethane combustion.

## B. SUMMARY OF THE MOST IMPORTANT RESULTS

### I. Numerical Simulation of Propellant Combustion with Detailed Chemical Kinetics

#### I.1 *Statement of Problem*

The purpose of this task is to establish a predictive model based on first principles for determining detailed ignition/combustion characteristics of energetic ingredients (including RDX and GAP) over a broad range of operating conditions. Both the gas- and condensed-phase processes are treated in depth, with the instantaneous propellant-burning rate and combustion wave structure calculated as part of the solution. Results have been validated against measured temperature and species-concentration profiles, as well as the pressure and temperature sensitivities of the burning rate.

#### I.2 *Summary of Most Important Results*

Several comprehensive numerical analyses have been developed to treat the detailed physical and chemical processes involved in nitramine-propellant and azide-binder combustion and ignition. The formulation is based on the complete conservation equations for both condensed and gas phases and takes into account finite-rate chemical kinetics and thermodynamic phase transition. Parametric studies have been conducted to investigate the detailed flame structures and burning behavior of RDX monopropellant and RDX/GAP pseudo-propellant under various initial and ambient conditions. The effect of external radiant energy deposition on propellant combustion was also examined systematically.

Figures 1.1 and 1.2 present detailed distributions of temperature and major species concentrations in both the gas-phase and subsurface regions for self-sustained RDX combustion at 1 atm. In spite of the nearly monotonic nature of the temperature field, a multi-stage chemical pathway is clearly identified. The overall reaction mechanisms globally consist of three steps: 1) decomposition of RDX into  $\text{CH}_2\text{O}$ ,  $\text{HCN}$ ,  $\text{NO}_2$ , etc. near the surface, 2) first-stage oxidization that includes formation of  $\text{NO}$  and  $\text{H}_2\text{O}$  as well as removal of  $\text{NO}_2$ , and 3) second-stage oxidization that includes conversion of  $\text{HCN}$  and  $\text{NO}$  to the final products such as  $\text{CO}$ ,  $\text{N}_2$ , and  $\text{H}_2$ . The analysis has been validated against experimental data and employed to calculate the propellant burning rates over a pressure range of 1-100 atm. The pressure exponent in the burning-rate law, i.e.,  $r_b = ap^n$ , is about 0.83, showing good agreement with measurements. Detailed discussions of the results are given in Refs. 1.1 and 1.2.

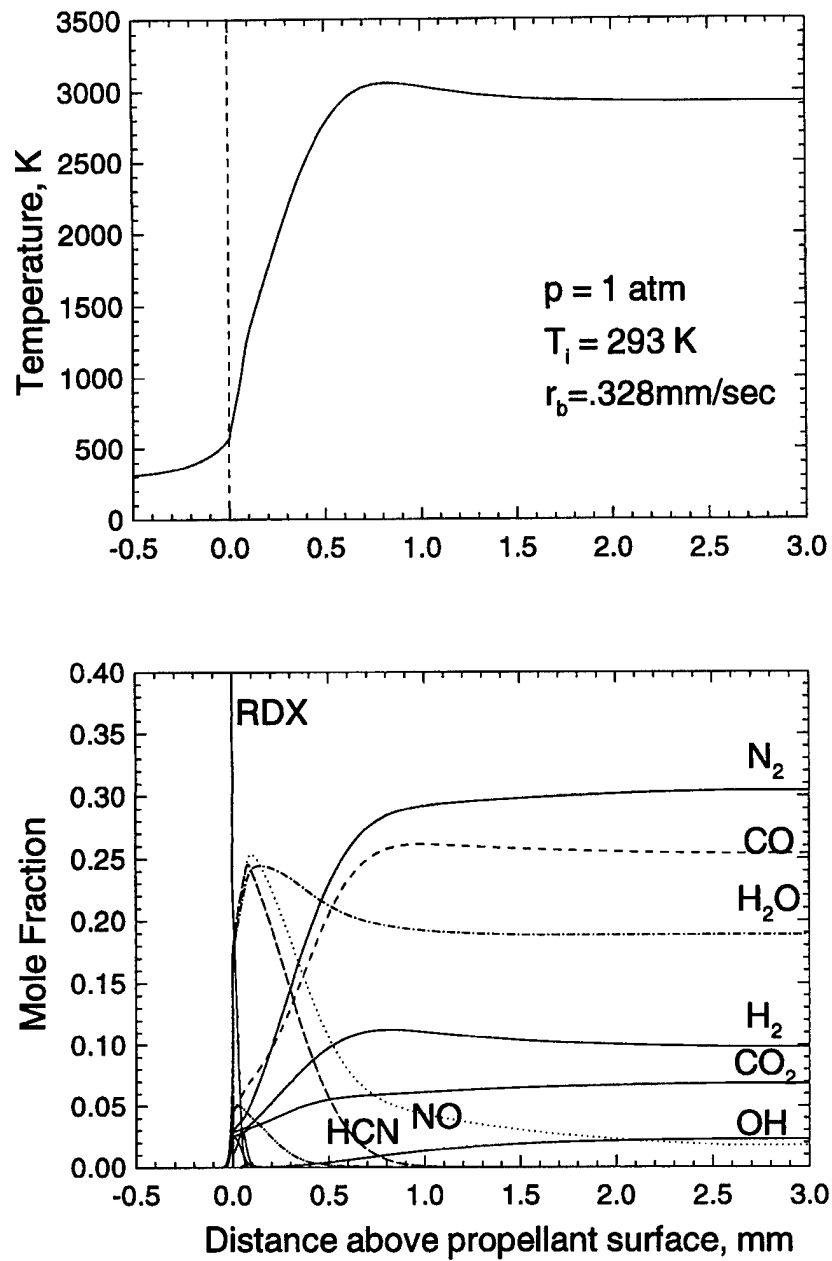


Figure 1.1 Distributions of temperature and major species concentrations of self-sustained RDX combustion at 1 atm.

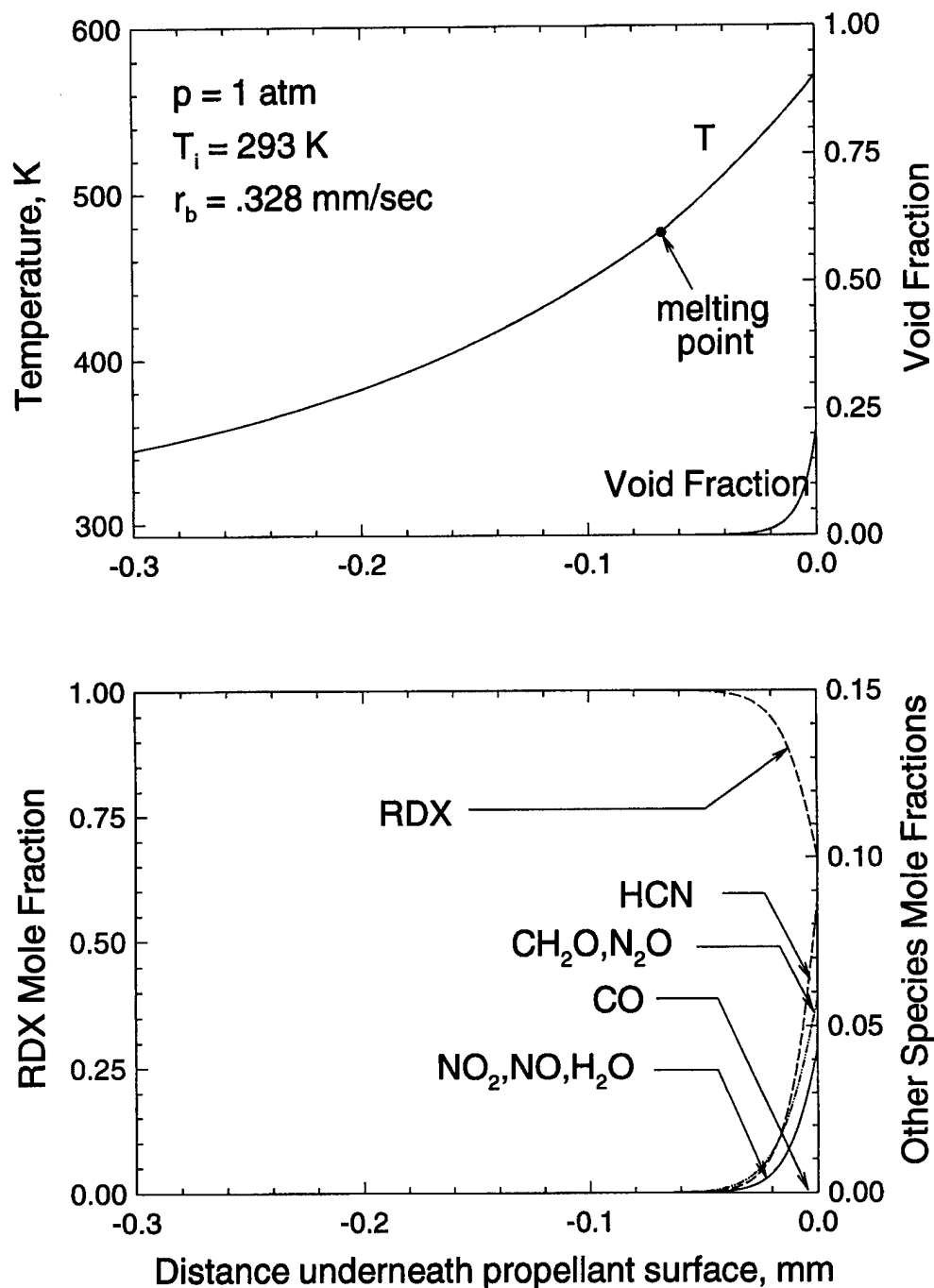


Figure 1.2 Close-up view of temperature and species-concentration profiles in subsurface region for self-sustained RDX combustion at 1 atm.

The combustion model for nitramine monopropellant was extended to include the effect of an azide binder such as GAP, AMMO, and BMMO. The formulation accommodates all essential physicochemical processes associated with azide-binder thermal decomposition and reactions. The chemical kinetic scheme accommodates seven global decomposition pathways of RDX and GAP and subsequent gas-product reactions in the near-surface multi-

phase layer. Vaporization of the melted propellant and the ensuing condensation process are also included to provide a complete description. The gas-phase kinetics scheme involves a total of 65 species and 418 reactions in order to obtain detailed flame structures and heat-release mechanisms. Figures 1.3 and 1.4 show the condensed- and gas-phase solutions of RDX/GAP propellant (mass fraction 4:1) combustion at 1 atm with a  $\text{CO}_2$  laser heat flux of  $100 \text{ W/cm}^2$ . A dark-zone temperature plateau around 1,200-1,400 K is clearly observed, in contrast to the situation with RDX monopropellant combustion without external heat flux. This phenomenon may be attributed to the higher burning rate due to the presence of GAP, which effectively stretches the flame. The model is the first and the most comprehensive of its kind to date, providing much useful information about the propellant burning mechanism. More comprehensive discussions of the model and results are given in Ref. 1.3.

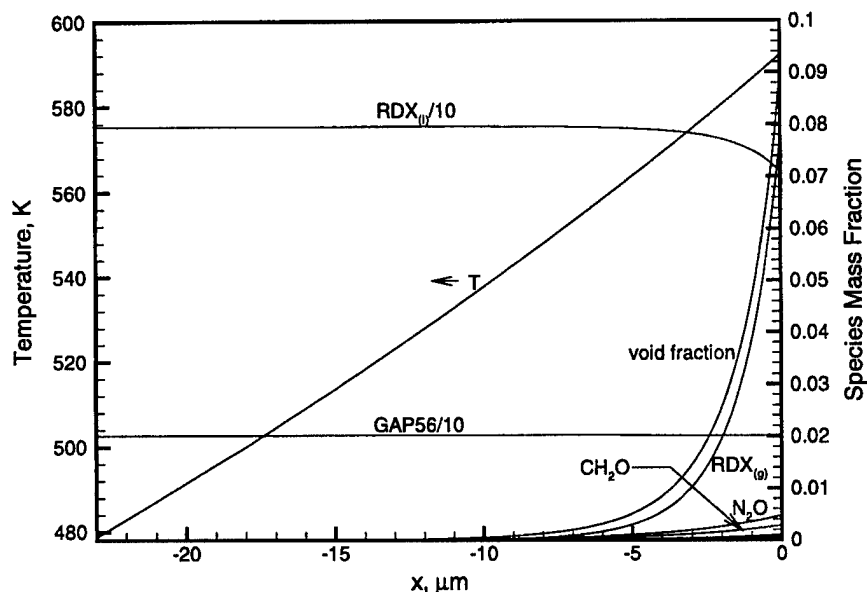


Figure 1.3 Temperature, void fraction, and species-concentration profiles in condensed phase for RDX/GAP pseudo-propellant combustion.

The analysis has also been applied to study the laser-induced ignition of RDX monopropellant. Detailed burning characteristics were investigated, with emphasis placed on the evolution of flame structure and ignition properties. Included as part of the results were ignition delay, onset of ignition kernel, and temporal evolution of the temperature and species concentration profiles. Several distinct ignition stages, including inert heating, pyrolysis, and flame occurrence and propagation, were identified. Figure 1.5 shows the predicted temperature profiles at various times for an incident heat flux of  $400 \text{ W/cm}^2$  at 1 atm. The calculated ignition delay and transient development of the temperature and species-concentration fields agree well with experimental data. A more detailed discussion is given in Refs. 1.4 and 1.5.

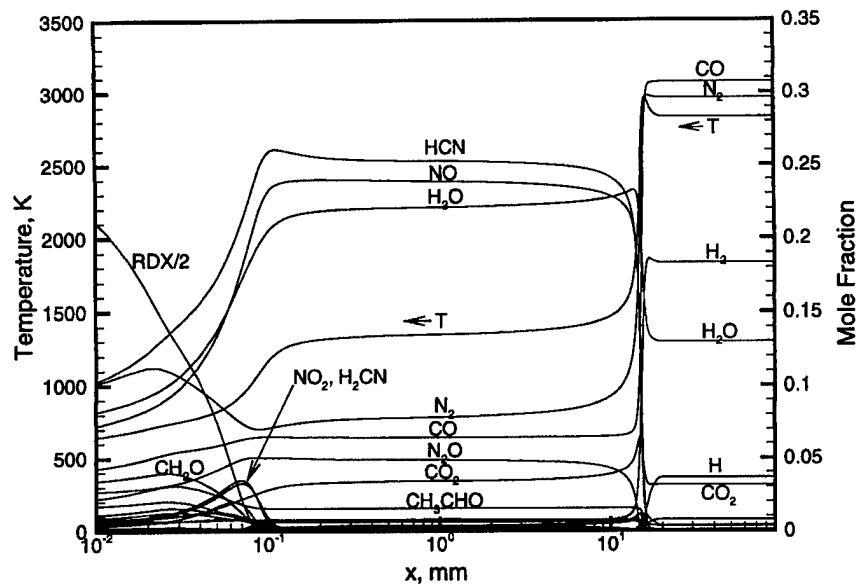


Figure 1.4 Temperature and species-concentration profiles in gas phase for RDX/GAP pseudo-propellant combustion.

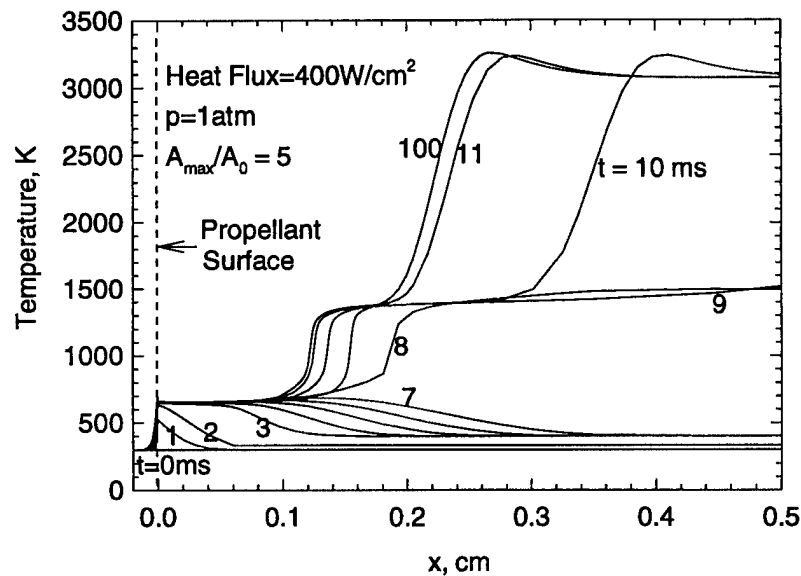


Figure 1.5 Predicted temperature profiles at various times for laser-induced ignition of RDX monopropellant at 1atm.

### I.3 References

- 1.1. Liao, Y.-C. and Yang, V., "Analysis of RDX Monopropellant Combustion with Two-Phase Subsurface Reactions," *Journal of Propulsion and Power*, Vol. 11, No. 4, July-August, 1995, pp. 729-739.
- 1.2. Liao, Y.-C. and Yang, V., "On the Existence of Dark-Zone Temperature Plateau in RDX Monopropellant Flame," AIAA Paper 97-0589, January, 1997.

- 1.3. Liao, Y.-C., Thynell, S.T., and Yang, V., "Analysis of RDX/GAP Propellant Combustion with Detailed Chemistry," presented at the JANNAF Combustion Subcommittee Meeting, October, 1997.
- 1.4. Yang, V., and Liao, Y.-C., "A Time-Accurate Analysis of RDX Monopropellant Combustion with Detailed Chemistry," Proceedings of the 32<sup>nd</sup> JANNAF Combustion Subcommittee Meeting, NASA Marshall Space Flight Center, Huntsville, Alabama, October 23-27, 1995. CPIA Publication 638, Vol. I, pp. 57-67, October, 1995.
- 1.5. Liao, Y.-C. and Yang, V., "An Improved Model of Laser-Induced Ignition of RDX Monopropellant," CPIA Publication 653, Vol. 2, pp. 529-545, 1996; 33rd JANNAF Subcommittee Meeting, Naval Postgraduate School, Monterey, CA, November 4-8, 1996.

## **II. Micro-probe Mass Spectrometer Studies of Propellant Flames**

### **II.1 *Statement of Problem***

These measurements were performed to obtain an understanding of the effects of propellant composition, pressure and heat flux on the species profiles within propellant flames. The species measurements were performed with a microprobe mass spectrometer system with a spatial resolution of approximately 100  $\mu\text{m}$ . In addition to the species measurements, temperatures within the propellants and in the gas-phase were measured with micro-thermocouples varying in size from 5 to 75  $\mu\text{m}$ . High magnification video was used to observe the sample and flame structure during combustion, and to determine the distance of the microprobe or the micro-thermocouple from the sample surface.

### **II.2 *Summary of Most Important Results***

Over the course of the URI program, a number of propellants and ingredients were investigated with  $\text{CO}_2$  laser heat fluxes ranging from 100 and 400  $\text{W}/\text{cm}^2$  and pressures from 0.5 to 3 atm. The ingredients investigated included RDX, CAB and ATEC as well as XM39 and M43 propellants. In addition, pseudo-propellants of RDX/CAB were studied to bridge the gap between propellants and pure RDX. The pellets were created by mixing the two ingredients and pressing them into pellets at pressures of approximately 2,500 atm. The major results from these studies are summarized in this section. Detailed results can be found in Refs. [2.1-2.4].

Ninety percent RDX was used in RDX/CAB pseudo propellants to bridge the gap in species and temperature data between the nitramine composites, such as XM39 (76% RDX), and pure RDX. This study showed the effects of binder on the surface temperature and gas-phase reactions or concentrations of stable species. Figure 2.1 shows the effect of CAB on the species profiles of  $\text{N}_2\text{O}$  and  $\text{NO}_2$  in the gas phase.

The complete consumption of  $\text{NO}_2$  indicates the end of the primary reaction zone. Figure 2.1 clearly shows that the addition of CAB stretches out the primary reaction zone. For RDX at 400  $\text{W}/\text{cm}^2$ , this zone exists up to 1 mm above the surface, while for RDX/CAB (90/10) it stretches out to about 2 mm above the propellant surface. The lower  $\text{NO}_2$  mole fraction at the surface of RDX/CAB is consistent with the fact that CAB does not contain any nitrogen. The surface temperature for RDX/CAB is about 600 K, which is about 10 - 20 degrees lower than that for RDX. Formation of  $\text{NO}_2$  is favored at higher temperatures, and the lower surface temperature is consistent with a lower  $\text{NO}_2$  concentration.

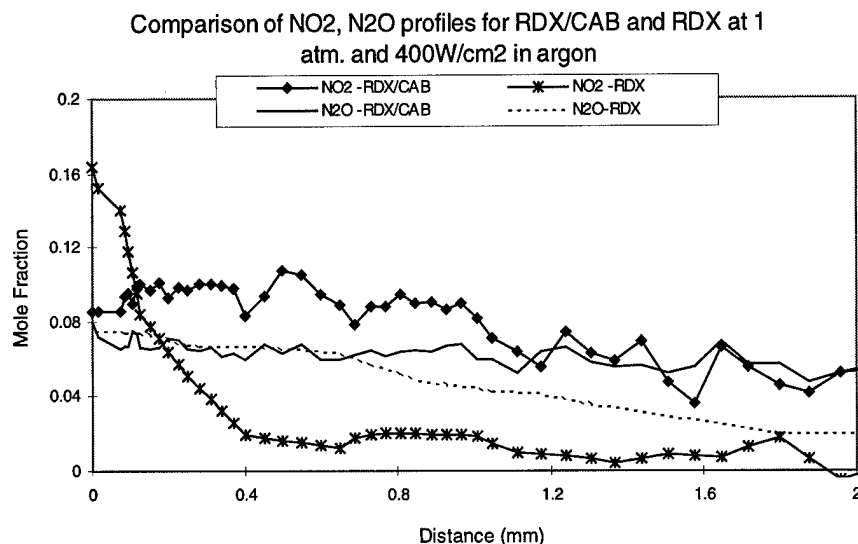


Figure 2.1 Comparison of NO<sub>2</sub> and N<sub>2</sub>O profiles for RDX and RDX/CAB at 1 atm and 400W/cm<sup>2</sup> in argon.

In the secondary flame region, N<sub>2</sub>O undergoes a reduction to form N<sub>2</sub>. The N<sub>2</sub>O profile for RDX/CAB remains fairly constant while the N<sub>2</sub>O profile for RDX shows a slow decay. This also suggests that the addition of the binder has stretched out the gas-phase reactions.

Figure 2.2 shows the temperature profiles for RDX, RDX/CAB, XM39 and M43 at 1 atm and an incident laser heat flux of 400W/cm<sup>2</sup> with argon as the ambient gas. The surface temperatures for XM39, M43 and RDX/CAB were 580, 592, and 600 K, respectively. In M43, an energetic plasticizer replaces the ATEC present in XM39, and this seems to result in a higher surface temperature. The energetic plasticizer also causes a faster temperature rise in the gas-phase region. M43 and XM39, when combusted in an argon environment, do not have a luminous flame region. The fuel-rich nature of these propellants prevents complete combustion in an inert environment. The temperature profiles show a rise from its surface value to a stable "dark zone" temperature plateau.

The higher percentage of RDX in the RDX/CAB pseudo propellant, as compared to XM39, raises the surface temperature. The temperature profile for RDX/CAB shows a plateau at about 1,450-1,500 K. The RDX temperature profile shows a monotonic rise to its final temperature of about 3,000 K. The final temperature for RDX/CAB is about 2,500 K. The addition of CAB seems to result in a "dark zone." The lower surface temperature for RDX/CAB may result from a simple dilution effect or that the CAB tends to slow the exothermic sub-surface reactions.

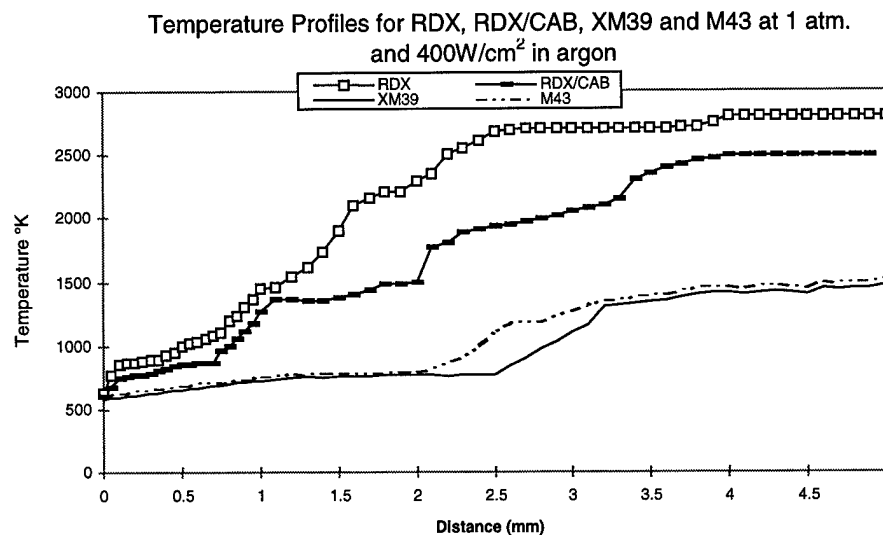


Figure 2.2 Temperature profiles for RDX, RDX/CAB, XM39 and M43 at 1 atm and 400W/cm<sup>2</sup> in argon.

Figure 2.3 shows a comparison between NO<sub>2</sub> and N<sub>2</sub>O profiles for XM39 and M43 at 1 atm with argon as the ambient gas. The RDX decomposition mechanism for NO<sub>2</sub> formation is favored at higher surface temperatures, and the higher surface mole fractions for NO<sub>2</sub> in M43 (23%) as compared to XM39 (20%) appear to be consistent with this mechanism.

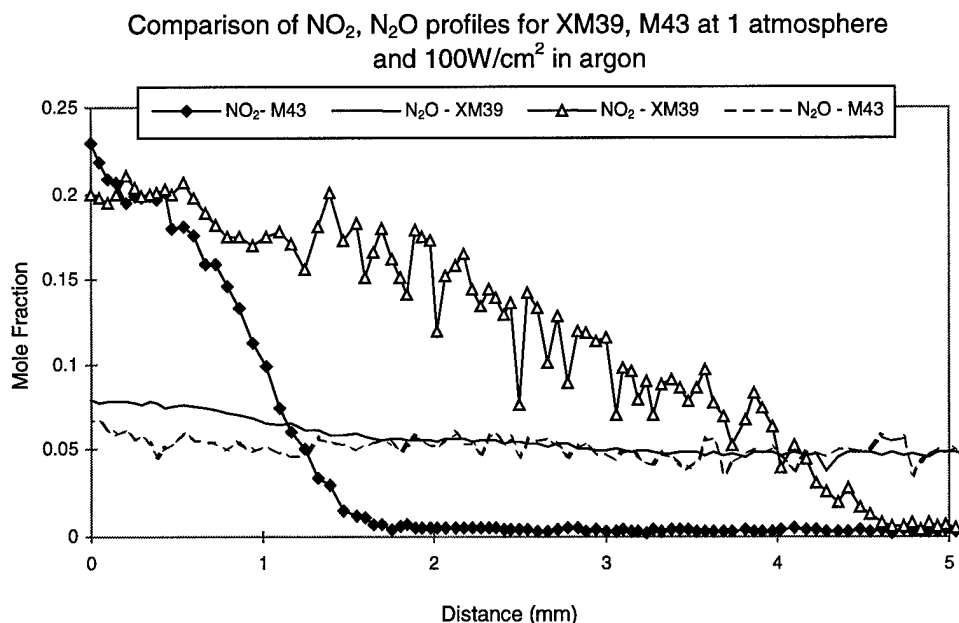


Figure 2.3 Comparison of NO<sub>2</sub>, N<sub>2</sub>O profiles for XM39 and M43 at 1 atm and 100W/cm<sup>2</sup> in argon.

The primary reaction zone, as defined by the complete consumption of NO<sub>2</sub>, is much shorter for M43 (1.6mm) as compared to XM39 (4.5 mm). The quicker consumption of NO<sub>2</sub> in the gas-phase of M43 is consistent with the faster temperature rise (Fig. 2.2). The lower surface

temperature for XM39 favors the reaction pathway that forms  $\text{CH}_2\text{O}/\text{N}_2\text{O}$ , and this is observed in the higher  $\text{N}_2\text{O}$  mole fraction for XM39 (8%), as compared to M43 (6%). In both cases, a final flame was absent and the propellants tended to “fizz burn”. The species profiles show the mole fractions stabilize into its “dark-zone” values.

When air is the ambient gas, XM39 shows a luminous flame and undergoes complete combustion to give final flame species and temperature. The fuel-rich nature of the composite propellants suggests that an oxidizer-rich environment is necessary for complete combustion. Figure 2.4 shows a comparison between CO and NO profiles for XM39 combustion in argon and air. The figure clearly illustrates the similarities in magnitude of mole fractions in air and argon in the near-surface region. The presence of air as the ambient gas allows complete combustion of XM39 and hence the higher temperatures to allow the NO to undergo a reduction reaction to form  $\text{N}_2$ . In the case of argon as the ambient gas, the NO mole fraction stabilizes at its dark-zone value. Similar behavior can be observed for the CO profile.

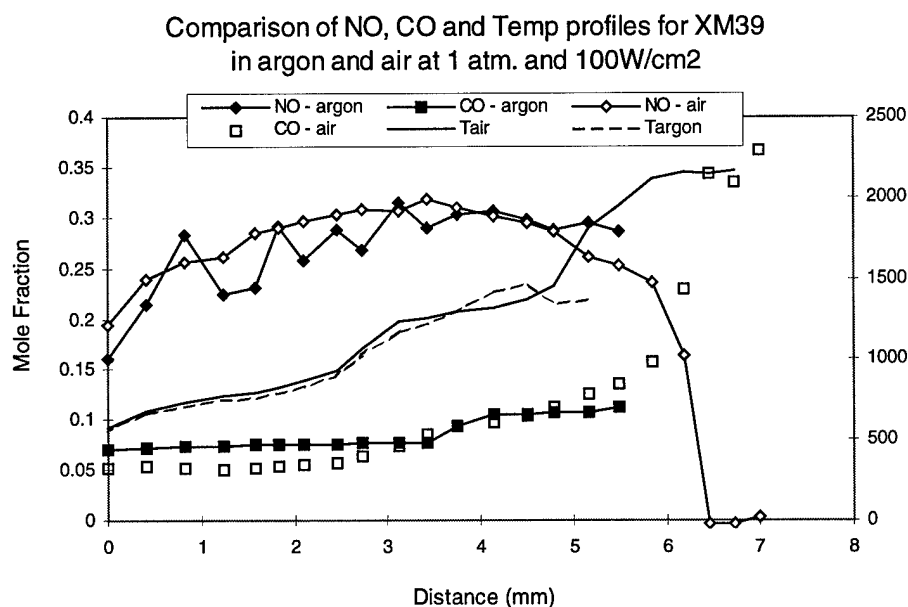


Figure 2.4 Comparison of CO, NO and temperature profiles for XM39 at 1 atm and 100W/cm<sup>2</sup> in argon and air.

The temperature profile shows remarkable similarity in values near and at the surface. This is consistent with the measured species profiles. Oxygen was also measured, and it showed little diffusion into the primary reaction zone. This again seems to suggest that the near-surface chemistry is independent of the ambient gas composition.

Table 2.1 shows that variation in heat flux changes the burn rate substantially but does not affect the surface temperature. The higher heat flux stretches out the gas-phase reaction regions but does not significantly alter the concentrations in the near-surface region. The temperature profiles in the gas-phase are also fairly consistent. This suggests that the radiative heating effect on surface chemistry is not significant. The surface and near-surface chemistry seem to be driven by the condensed-phase reactions.

Table 2.1 Burn rate and surface temperature data for various propellants at 1 atm in argon.

Propellant	Burn Rate (mm/s)		Surface Temperature (K)	
	100W/cm <sup>2</sup>	400W/cm <sup>2</sup>	100W/cm <sup>2</sup>	400W/cm <sup>2</sup>
XM39	0.6	1.1	575	580
M43	0.65	1.2	585	592
RDX	-	1.4	-	620
RDX/CAB	-	1.32	-	600

### II.3 References

- 2.1 Kudva, G., C.-J. Tang, Y.-J. Lee, and T.A. Litzinger, "A Study of the Effects of Pressure Variations on the Deflagration of RDX Composite Propellants," Proceedings of the 32nd JANNAF Combustion Subcommittee Meeting, NASA Marshall Space Flight Center, Huntsville, Alabama, October 23-27, 1995. CPIA Publication 638, Vol. I, pp. 161-171, October, 1995.
- 2.2 Kudva, G., C.-J. Tang, Y.-J. Lee, and T.A. Litzinger, "Study of Laser-Assisted Combustion of RDX-CAB Pseudo-Propellants at Various Operating Conditions," CPIA Publication 653, Vol. 2, pp. 569-578, 1996; 33rd JANNAF Subcommittee Meeting, Naval Postgraduate School, Monterey, CA, November 4-8, 1996.
- 2.3 Y.-J. Lee, C.-J. Tang, and T.A. Litzinger, "A Study of Gas-Phase Processes During the Deflagration of RDX Composite Propellants Using a Triple Quadrupole Mass Spectrometer," 31st JANNAF Comb. Subcommittee Meeting, October 17-21, 1994, Sunnyvale, CA, CPIA Public. 620, Vol. II, pp. 425-437.
- 2.4 Kudva, G., C.-J. Tang, Y.-J. Lee, and T.A. Litzinger, "Study of Laser-Assisted Combustion of Nitramine Propellants," presented at the Eastern States Section of the Combustion Institute, 1996 Fall Technical Meeting, Hilton Head, SC, December, 1996.

## III. FTIR Absorption Spectrometry of Propellant Flames

### III.1 Statement of Problem

This part of the project deals with the development of a non-intrusive diagnostic technique for the determination of temperature and species profiles within solid-propellant flames at elevated pressures. Such data are pertinent to model validation. The experimental technique employed a Fourier transform infrared (FTIR) spectrometer, which acquires spectral data along a line-of-sight (LOS). A high-pressure chamber was designed and constructed, which allows observation of the flame zone, translation of the propellant strand, pressure control, and measurement of condensed- and gas-phase temperatures using fine-wire thermocouples.<sup>3.1-3.3</sup> The major difficulty to overcome in the data-reduction procedure is to account for a variation of temperature and species along the line-of-sight. As shown in Fig. 3.1, the purge gas interacts with the flame zone to create a radially varying distribution of temperature and species. At a certain distance above the burning surface, the radial variation could be significant.

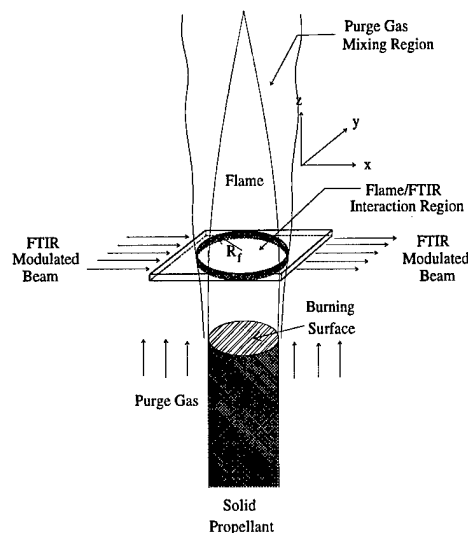


Figure 3.1 Schematic diagram of the FTIR beam propagation through the solid-propellant flame.

### III.2 Summary of Most Important Results

A data-reduction algorithm was developed to account for radial variation of temperature and species concentrations.<sup>3,4-3.5</sup> A discussion of the effect of noise in spectra, use of different spectral regions, instrument line shape and IR-active molecules is available.<sup>3,4-3.5</sup> Here, we summarize its application on the determination of centerline temperature and species mole fractions by using FTIR spectra acquired during steady-state combustion of XM39. The fundamental band of CO is first used to determine LOS-average, and second, radial variations in temperature and CO partial pressure. The deduced temperatures are then used to determine the partial pressures of other IR-active species.

*Temperature Measurements* - Temperatures deduced from FTIR spectra are compared to thermocouple measurements (S-type) in Figs. 3.2 and 3.3 for steady-state combustion of XM39 at 15 and 22 atm, respectively.<sup>3,6</sup> The closed-faced symbols are LOS-average values, the open-faced symbols are centerline values from sixth-order power series approximation for the radial temperature profiles, and the lines represent thermocouple data. Four FTIR tests at 15 atm and two tests at 22 atm are shown to demonstrate the reproducibility. Figure 3.2 shows that the LOS-average temperatures are within 70 K of the thermocouple traces near the surface (less than 3 mm from the surface), whereas the LOS-average values are 200 to 300 K lower than those acquired by thermocouples further from the surface.

LOS-average and centerline temperatures both match the thermocouple readings near the surface, where the mixing region is small. The data-reduction algorithm provided a good fit to the spectra acquired near the surface, as indicated by the value of  $\chi^2$  and a visual comparison between the measured and fitted spectra. Further from the surface, the mixing region grows, causing the LOS-average temperature to be significantly different from thermocouple measurements. In this region of the flame, the use of LOS-average temperatures and partial pressures within the algorithm resulted in poor fits (based on  $\chi^2$ ) to

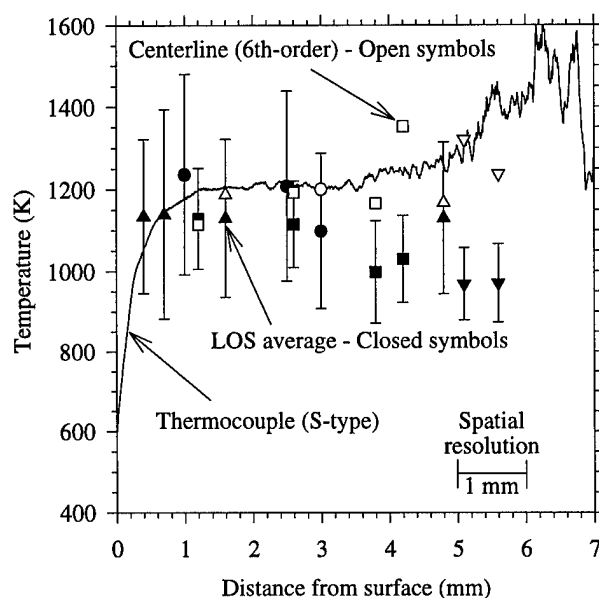


Fig. 3.2 Temperature profiles of an XM39 propellant flame at 15 atm using FTIR spectroscopy and Pt/Pt-10 % Rh (S-type) thermocouple.

the acquired spectra. However, the centerline values from deduced sixth-order power series profiles reproduce the thermocouple trace. Error bars (95 % confidence limits) on the LOS-average values were computed. Estimates of noise within the CO transmittance data were made using the data-reduction analysis and measured noise from the 2,500 to 2,600  $\text{cm}^{-1}$  range. Temperatures and CO partial pressures were determined from CO spectra over the spectral range from 2,000 to 2,090  $\text{cm}^{-1}$ . The lower limit was chosen to minimize interference from NO, while the upper limit was chosen to minimize the number of transitions employed.<sup>3,6</sup>

Tests performed at 22 atm show a dark zone, varying in length from 0.5 to 2.0 mm. This variation in length, coupled with a slightly uneven burning surface with respect to the FTIR beam, leads to vertical variations within the probe volume. The vertical variations are noticeable in FTIR spectra taken near the surface, where high-temperature CO transitions are observed in the low-temperature NO band structure, as well as in recorded images taken during combustion. Only LOS-average values were determined at this pressure. Beyond 2 mm from the surface, LOS-average temperatures are within 100 K of the thermocouple traces. The LOS-average values determined below 2 mm strongly depend on the species and spectral ranges used for data reduction. The 1,950 to 2,030  $\text{cm}^{-1}$  range was used to determine temperatures and CO partial pressures above 2 mm. Interference from NO is small at high temperatures allowing a spectral region which is more sensitive to high-temperature CO transitions to be used by the algorithm. Flame temperatures obtained by thermocouples and the data-reduction technique are slightly lower than the adiabatic flame temperature of 2,163 K for XM39 at 22 atm. Radiative heat losses may play a role since burn rates are low (long residence time) and the flame is luminous.

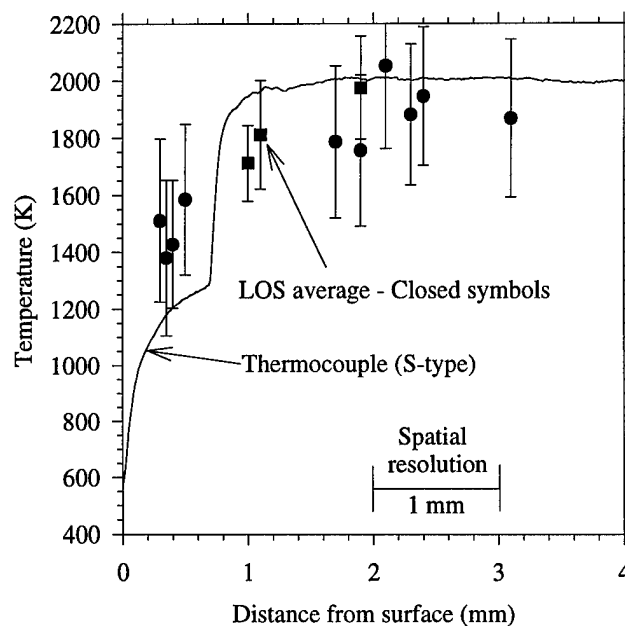


Fig. 3.3 Temperature profiles of an XM39 propellant flame at 22 atm using FTIR spectroscopy and Pt/Pt-10 % Rh (S-type) thermocouple.

*Species Measurements* - Figure 3.4 shows the deduced CO and NO mole-fraction profiles of the XM39 flame at 15 atm. Within this figure, the closed-faced symbols are LOS-averaged values whereas the open-faced symbols are centerline values from sixth-order power series approximations for the radial profiles of species and temperature. CO mole fractions and temperatures were deduced from the FTIR spectra using the spectral range from 2,000 to 2,090  $\text{cm}^{-1}$ , whereas NO mole fractions were determined using the spectral range from 1,880 to 1,950  $\text{cm}^{-1}$ . The narrow vibrational band width and lack of radiative properties beyond 1,950  $\text{cm}^{-1}$  for NO dictated the use of this spectral range, which is sensitive to high and low temperature rovibrational transitions. Close to the surface ( $< 3$  mm), no significant corrections for spatial variations in CO mole fractions were determined from the spectral transmittance measurements, and therefore, only LOS-average values are shown in this region in Fig. 3.4. Beyond 3 mm, spatial variations in NO and CO mole fractions were found from spectral transmittance measurements using the data-reduction algorithm. Centerline values of CO mole fractions using the sixth-order power series were larger than LOS-average values, whereas corrected NO mole fractions were slightly lower than the LOS-average values. The algorithm is able to use the spectral variations in transmittance to correct for spatial variations in CO and NO. In Fig. 3.4, 95% confidence limits on the LOS values were also calculated.<sup>3,6</sup>

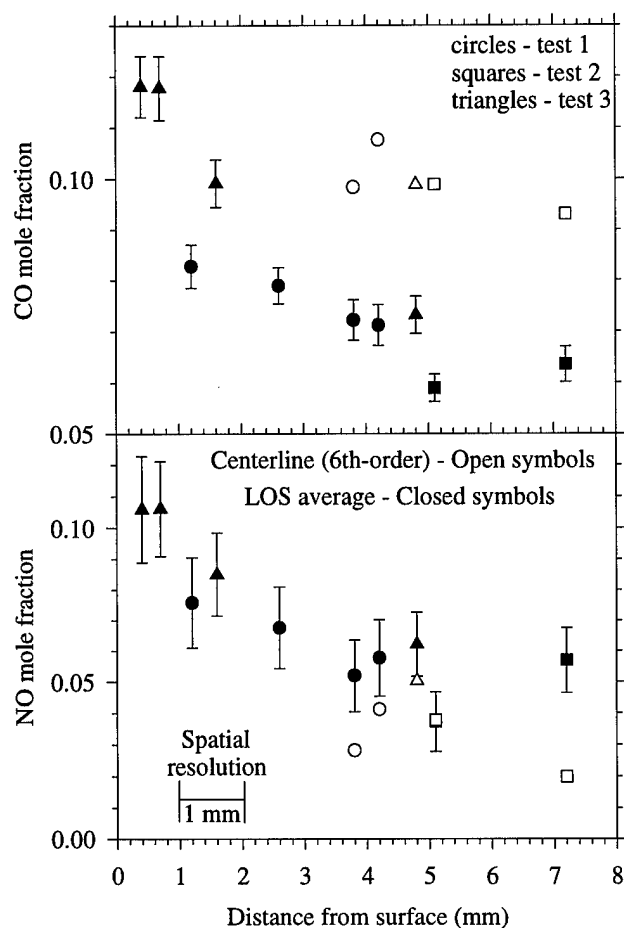


Figure 3.4 Deduced CO and NO mole-fraction profiles of an XM39 flame at 15 atm.

The FTIR spectra also indicated the presence of  $\text{CO}_2$ ,  $\text{N}_2\text{O}$ ,  $\text{H}_2\text{O}$ ,  $\text{HCN}$ , and  $\text{CH}_4$ . LOS-average mole fractions of these species were found close to the surface. Further from the surface, the algorithm was not able to determine radial profiles for these molecules. This inability is attributed to the lack of accurate high-temperature radiative properties.

Much additional work needs to be conducted to fully exploit the developed data-reduction technique. The major disadvantage is the lack of radiative properties at high temperatures. This involves the determination of line strength, transition frequencies, and the dependence of the pressure broadened half-width on temperature, pressure, and the partial pressures of other combustion products. Such data are also of interest in plume calculations. In addition, accurate models of line-mixing and sub-Lorentzian behavior of rovibrational lines are also needed to accurately determine spatial variations in temperature and species partial pressure from spectral transmittances.

### III.3 References

- 3.1 Mallery, C.F., E. Kim, and S.T. Thynell, "High-pressure Strand Burner System for Propellant Flame Studies Using Absorption Spectroscopy," *Review of Scientific Instruments*, Vol. 66, No. 8, pp. 4091-4094, 1995.

- 3.2 Mallery, C.F., and S.T. Thynell, "Further Improvements to FTIR Absorption Spectroscopy of Propellant Flames for Profiling of Species and Temperature," Proceedings of the 32nd JANNAF Combustion Subcommittee Meeting, NASA Marshall Space Flight Center, Huntsville, Alabama, October 23-27, 1995. CPIA Publication 631, Vol. I, pp. 449-460, October, 1995.
- 3.3 Mallery, C.F., and S.T. Thynell, "Species and Temperature Profiles of Propellant Flames Obtained from FTIR Absorption Spectrometry," *Combustion Science and Technology*, Vol. 122, pp. 113-129, 1997.
- 3.4 Mallery, C.F., and S.T. Thynell, "Line-of-Sight Temperature and Species Profiles Determined from Spectral Transmittances," *J. Thermophysics and Heat Transfer*, Vol. 11, No. 3, pp.367-374, 1997.
- 3.5 Mallery, C.F., and S.T. Thynell, "Radial Temperature and Species Profiles from an Inverse Analysis of Spectral Transmittances," AIAA-paper 97-0120 presented at the 35th Aerospace Sciences Meeting, Reno, Nevada, (January 8-11, 1997); CPIA Publication 653, Vol. 2, pp. 371-382, 1996; presented at the 1996 JANNAF Combustion Subcommittee Meeting, Naval Postgraduate School, Monterey, CA, November 4-8, 1996.
- 3.6 Mallery, C.F., and S.T. Thynell, "Line-of-Sight Profiling of Temperature and Species in Propellant Flames Using FTIR Spectroscopy," Proceedings of the 34th JANNAF Combustion Subcommittee Meeting, West Palm Beach, Florida, October 27-31, 1997; also AIAA Paper 98-3827, presented at the 34th AIAA/ASME/SAE/ASEE Joint Propulsion Conference and Exhibit, July 12-15, 1998, Cleveland, OH.

#### **IV. Ignition Delay, Temperature Sensitivity, and UV/Visible Absorption Spectroscopy Measurements of Solid Propellants**

##### **IV.1 Statement of Problem**

During this research investigation, the flame structures of five different propellants, (namely JA-2, M9, M10, XM39, M43), pure RDX, and three RDX-based pseudo propellants containing different amounts of CAB binder were characterized. The specific objectives of this investigation are: 1) to provide experimental data on burning rates, ignition delay times, temperature and species (OH and NO) concentration profiles of solid propellants for guiding model development and validation, 2) to observe the ignition and combustion behavior of these propellants, 3) to determine the effect of percentage of CAB on the ignition and combustion processes of RDX/CAB pseudo propellants, and 4) to examine the pressure dependency of final flame temperatures and OH and NO mole fractions.

##### **IV.2 Summary of Most Important Results**

*UV/Visible Absorption Spectroscopy* - Absorption spectroscopy was used as the diagnostic technique to measure the gas-phase temperature and OH and NO concentration profiles of propellants. Absorption spectroscopy is a non-intrusive optical diagnostic technique for simultaneous determination of temperature and absolute concentration of chemical species from one measured spectrum. Application of this technique to solid propellant flames at low to intermediate pressures (up to 2 MPa) has recently been shown to be an effective and accurate method by A. J. Kotlar and J. A. Vanderhoff of ARL<sup>4.1</sup> and T. P. Parr of NAWC.<sup>4.2</sup> Although it is a simple and relatively inexpensive technique, it has sufficient sensitivity even for the detection of transient species with low concentrations in the flame zone.<sup>4.2</sup>

Absorption spectroscopy does not suffer from the collisional quenching effect, which is a major limitation for other linear optical techniques, such as laser induced fluorescence (LIF), especially at higher pressures.<sup>4.3</sup> The basic limitation of absorption spectroscopy is that it is a line-of-sight measurement method which is most suitable for one-dimensional flame-zone structure. When the flame structure is not one-dimensional, determination of the effective pathlength of the light beam becomes very difficult which in turn causes discrepancies in the deduced species concentration since assumed pathlength and species concentration are almost inversely proportional.<sup>4.4</sup>

The optical setup for UV/Visible absorption measurements was established and tested with high spatial resolution and signal-to-noise ratio.<sup>4.5</sup> A high-pressure, windowed test rig for propellant flame diagnostics and burn rate measurements was constructed. The test chamber was also upgraded to incorporate a propellant feeding mechanism using a computer-controlled linear actuator system. A 50-Watt CO<sub>2</sub> laser was employed for igniting the propellant sample. A surge tank was used in conjunction with the test chamber to maintain steadiness of the chamber pressure. Major characteristics of this setup include: high spatial resolution (up to 50  $\mu\text{m}$ ), capability of high-pressure measurement (up to 60 MPa), nearly constant pressure operation (less than  $\pm 1.5\%$  pressure variation), chamber purge for clear optical access, laser or nichrome wire ignition, and very accurate propellant feeding mechanism (0.1  $\mu\text{m}$  axial displacement per rotation step).<sup>4.4, 4.5</sup> An in-situ propellant heating system was also constructed to stretch the flame-zone height and thus enhance the optical diagnostics.

For JA-2 propellant, which is made of NC (59.5% by weight)/NG (14.9%)/DEGDN (24.8%)/others (0.8%), OH absorption measurements were conducted at pressures of 200, 500, 800, and 1000 psig to investigate the effect of pressure on the JA-2 flame.<sup>4.5</sup> This study represents the first attempt of absorption measurements of solid propellants above 300 psig. The deduced flame temperature in the luminous region showed a slight increase from 2,754 K at 200 psig to 2,873 K at 1,000 psig, which agrees well with the equilibrium calculations at respective pressures as shown in Table 4.1. The measured OH number density increased with pressure; however, the mole fraction of OH decreased with increasing pressure. This is believed to be associated with the increase in the total number of gaseous molecules at higher pressures. The measured OH concentrations were found to be lower than those from equilibrium calculations. A similar discrepancy was also observed by Vanderhoff et al.<sup>4.1</sup> of ARL and was attributed to both the highly nonlinear dependency of OH concentration on flame temperature and variations of local flame stoichiometry. In addition, effects of both heat and mass transfers between the flame and the environment also make the averaged, line-of-sight OH concentrations less than that near the central region of the flame. Furthermore, there are some uncertainties in the equilibrium calculations due to variations of reported thermochemical data of JA-2 ingredients. The propellant heater installed in the high-pressure windowed combustion chamber was used to increase the initial temperature of JA-2 by heating the purge gas. Increasing the initial propellant temperature stretches the flame zone, aiding in the resolution of the flame structure at high pressures when the flame structure would otherwise be extremely compact. The amount of flame zone stretching depends on the temperature sensitivity of the propellant. Even for JA-2, which has a very low temperature sensitivity, the visible dark zone at a pressure of 200 psig has been shown to

increase approximately 35% with an increase of initial temperature from 29 to 120°C.<sup>4,6</sup> Flame zone stretching by this technique has not been previously conducted by any other researchers working on solid propellants.

Table 4.1 Flame temperatures and OH concentration of JA-2 propellant at different pressures.

Pressure	Luminous Flame Temperature (K)	Equilibrium Calculation $T_f$ (K)	OH Number Density (molec./cm <sup>3</sup> ) $\times 10^{-17}$	OH Mole Fraction $\times 10^3$	Equilibrium OH Mole Fraction $\times 10^3$
1.60 MPa (217 psig)	2754 $\pm 124$	2822	1.09 $\pm 0.34$	2.81 $\pm 0.30$	5.65
3.55 MPa (500 psig)	2836 $\pm 147$	2844	2.31 $\pm 0.48$	2.61 $\pm 0.41$	4.22
5.62 MPa (800 psig)	2852 $\pm 179$	2855	3.31 $\pm 0.27$	2.32 $\pm 0.19$	3.52
6.99 MPa (1000 psig)	2873 $\pm 188$	2859	3.44 $\pm 0.30$	1.95 $\pm 0.17$	3.22

Temperature and NO concentration profiles of M43 and XM39 propellants showed plateaus when a spatially uniform dark zone existed between the burning surface and luminous flame regions.<sup>4,4,4,6</sup> Under this situation, M43 and XM39 have similar dark-zone temperatures (around 1,050 K for M43 and 1,150 K for XM39). However, M43 has at least 5 to 6% more of NO mole fraction than XM39 in the dark-zone region, indicating less conversion of NO<sub>2</sub> to NO in the primary reaction zone near the burning surface. Figure 4.1 shows a plot of temperature and NO concentration profiles of M43 propellant flame at 1.60 MPa when there were no flamelet attachments to the burning surface. However, in most tests, the luminous flame was attached to the burning surface through several flamelets.<sup>4,4,4,6</sup> When these luminous flamelets were attached to the burning surface, line-of-sight averaged NO concentrations (where a uniform pathlength is used in data analysis) exhibited a rapid reduction for increased distance from the burning surface. This reduction is caused by a shorter intercepted distance by the UV light beam in the dark zone as the vertical distance from the burning surface increases, and the deduced NO concentration is thereby decreased if the whole propellant diameter is used as the pathlength in the data analysis. Because flamelet attachment is inevitable for most solid propellants, spatially averaged quasi 1-D solid-propellant combustion models should take this aspect of flame into consideration. Thus, the data reported in this work should be very useful for theoretical model validations and improvements.

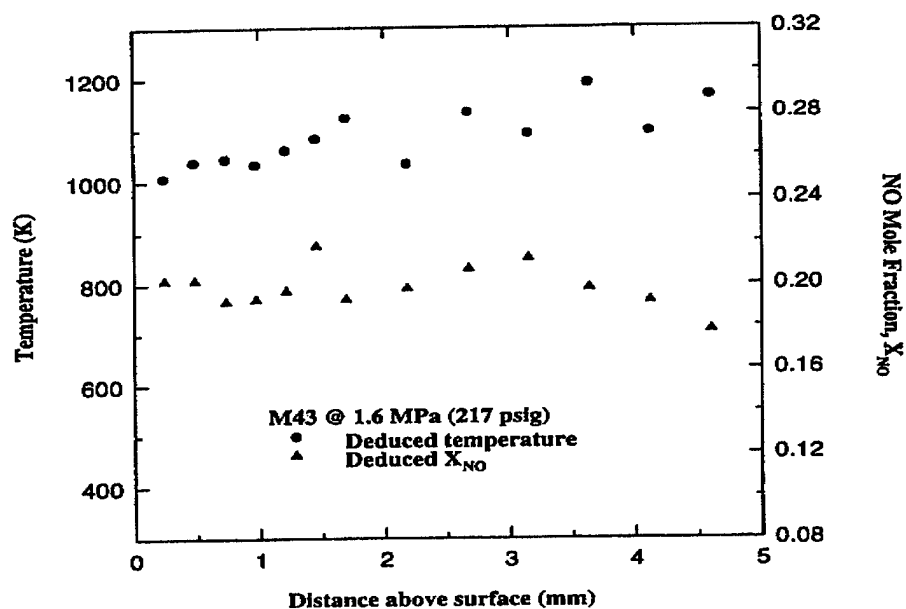


Figure 4.1. Temperature and NO concentration profiles for M43 propellant at 1.6 MPa.

The flame structures of pure RDX and RDX-based pseudo propellants containing different amounts of CAB binder were investigated to provide data for validating advanced combustion models for composite propellants.<sup>4,4,4,6-4,11</sup> The model simulation of pseudo propellants containing a few ingredients is easier than that of composite propellants with many ingredients because of complex physicochemical interactions between the ingredients. UV/Visible absorption measurements provided the profiles of gas-phase temperature and OH concentration of pure RDX and pseudo propellants containing RDX with CAB binder having 8%, 11%, and 14% by weight. OH absorption measurements for pure RDX and the three pseudo propellants were conducted at 0.45 MPa (50 psig). For pure RDX, tests were also conducted at two other pressures [0.17 and 0.79 MPa (10 and 100 psig)] to examine the effect of pressure on temperature and OH concentration. Tests were conducted with RDX/CAB (84/16) pseudo propellant; however, no adequate OH absorption was detected due to the low concentration of OH molecules at low flame temperature conditions. It was found that the flame structures of pure RDX and RDX/CAB pseudo propellants are quite different. Pure RDX has a highly non-one-dimensional flame structure, i.e., there were several bright columns of flame (flamelets) surrounded by a less luminous zone, whereas RDX/CAB pseudo-propellant flames are much more uniform than that of pure RDX mostly due to the reduced interaction between the gaseous flame and surface reaction zone. As the CAB percentage increases, the luminosity of the flame drastically decreases. For RDX/CAB (86/14) pseudo propellant, the flame is almost invisible during most of the test time. During this series of tests, unlike XM39 and M43 propellants, no multi-stage flame structures were observed for both pure RDX and RDX/CAB pseudo propellants processed by the shock-precipitation procedure.<sup>4,8,4,10,4,11</sup> This difference could be caused by the effect of other ingredients not included in the pseudo propellants. The deduced final-flame temperatures at 0.45 MPa from absorption spectroscopy measurements indicated a monotonic decrease of  $T_f$  with an increase of CAB percentage from 3,062 K for pure RDX to 2,742 K for RDX/CAB

(86/14%), as departure from stoichiometry became larger. Figures 4.2 and 4.3 show the temperature and OH concentration profiles of pure RDX and RDX/CAB (86/14) flames at 0.45 MPa, respectively. Similar figures were obtained for other pseudo propellants at 0.45 MPa and for pure RDX at 0.17 and 0.79 MPa. In Fig. 4.2, the temperature and OH concentration increase very rapidly to their maximum values at a position very close to the burning surface. In Fig. 4.3, the decreasing trend of the temperature and OH concentration in the luminous region is due mainly to the heat- and mass-transfer processes between the flame and the purge gas. Based on this series of measurements, the flame temperatures of pure RDX and three pseudo propellants were found to be very close to the calculated equilibrium temperatures. The deduced OH concentrations were lower than the equilibrium values due mainly to the non-one-dimensional nature of the pure RDX flame and uncertainties in the pathlength of the light beam. It is interesting to note that the flame heights, determined from the peak OH concentration locations, increase with the increase of the percentage of CAB in the RDX/CAB pseudo propellants. This increase is caused by a greater distance required for complete reactions of decomposed fragments of CAB and RDX. The CAB decomposition is endothermic and absorbs more energy from the propellant when its percentage increases.

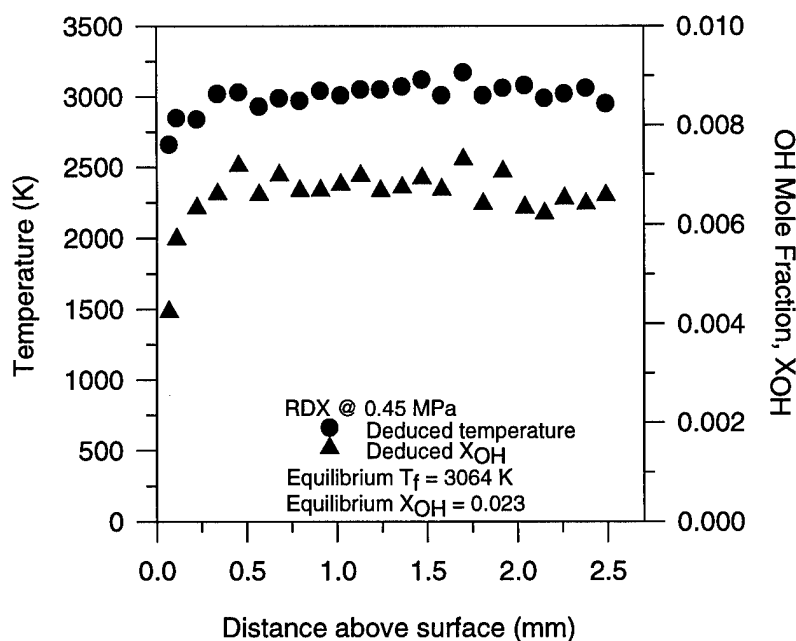


Figure 4.2 Deduced gas-phase temperature and OH mole fraction profiles of RDX flame at 0.45 MPa.

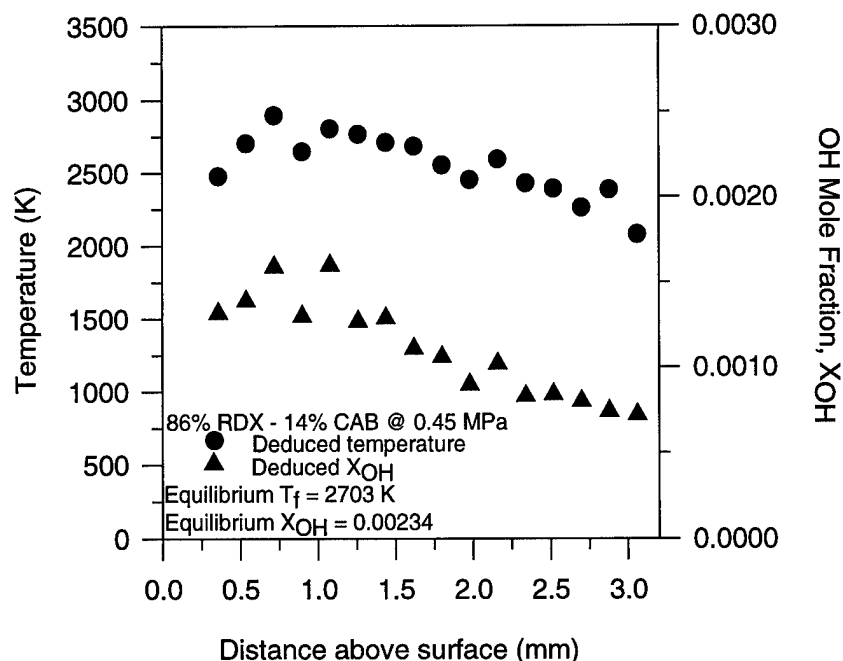


Figure 4.3 Deduced gas-phase temperature and OH mole fraction profiles of RDX/CAB (86/14%) flame at 0.45 MPa.

*Temperature Sensitivity* - Burning rates of pure RDX and three RDX/CAB pseudo propellants were determined from video records. At 0.45 MPa, the burning rates of pseudo propellants were fitted into the following equation:

$$r_b \text{ (mm/s)} = 0.9543 - 0.029 \times [\text{weight \% CAB}]$$

Burning rates of pure RDX as a function of pressure were fitted into the equation  $r_b = a P^n$  with  $n = 0.836 \pm 0.002$  and  $a = 1.850 \pm 0.002$ .

The measured burning rates of pure RDX at 25 and 120°C were compared with the calculated results of Liao and Yang of PSU and the room-temperature data of M. S. Miller of ARL for military grade RDX in Fig. 4.4. It is interesting to note that the burning rate data of military grade RDX which contains up to 10% HMX impurity of Miller is substantially higher than the pure RDX. This implies that the combustion of XM39 and M43 propellants with military grade RDX could have non-negligible influence of HMX to their burning rates. Also it would be useful to simulate the combustion behavior of military grade RDX numerically. From these measured burning rate data, the temperature sensitivity of pure RDX was found to be a linear function of pressure according to the following equation:

$$\sigma_p \text{ (1/K)} = -0.000391 + 0.00289 P \text{ (MPa)}$$

The value of  $\sigma_p$  changed from 0.000137 to 0.00192 K<sup>-1</sup> when the pressure was increased from 0.17 to 0.79 MPa.

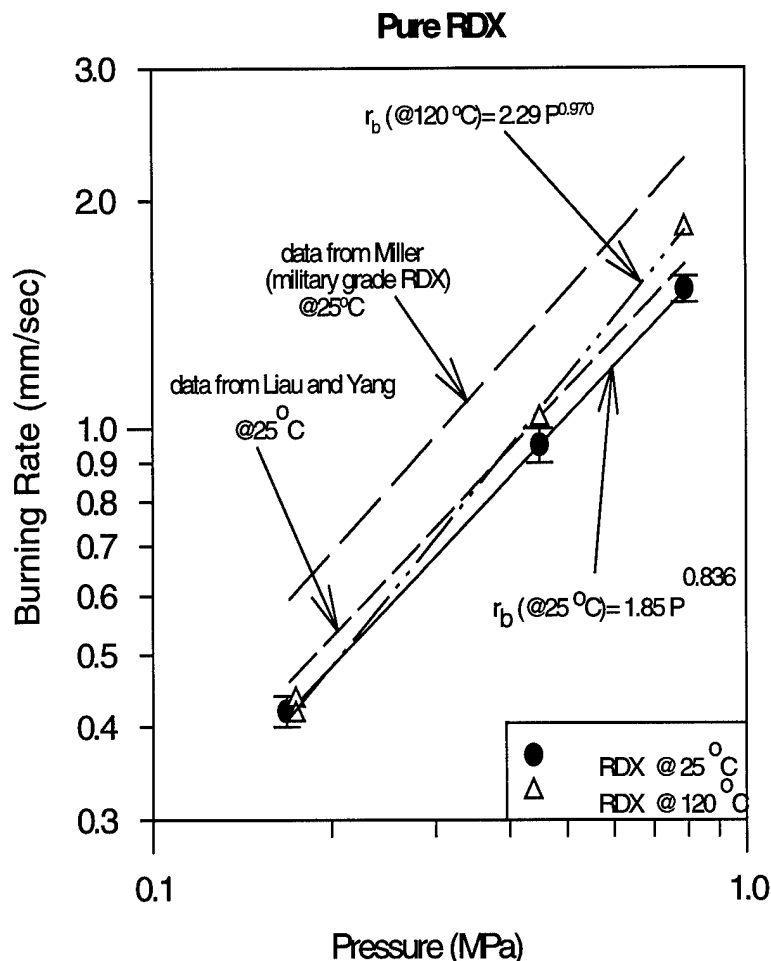


Figure 4.4 Burning rates of pure RDX as a function of pressure and initial temperature.

**Ignition Delay** - Ignition delay is one of the most important parameters in the characterization of propellant ignition behavior. In this study, ignition delay times of the pure RDX, pure HMX, and three RDX/CAB pseudo propellants were determined under various levels of incident  $\text{CO}_2$  laser energy fluxes at 0.45 MPa.<sup>4,8,4.10,4.11</sup> In this part of the investigation, ignition delay times based upon the onset of light emission ( $t_{LE}$ ) and gas evolution ( $t_{GE}$ ) were determined as a function of incident energy flux. The self-sustained Go/No-Go ignition boundaries (defined as  $t_{ign}$ ) for these propellants were also obtained. These ignition data are very useful for model validation. A CCD video camera system with a framing rate of 60 frames/s was used to record the ignition phenomena. Figures 4.5 to 4.7 show the measured delay times ( $t_{LE}$  and  $t_{GE}$ ) as well as Go/No-Go boundary ( $t_{ign}$ ) with respect to average incident laser energy fluxes of the pure RDX, pure HMX, and RDX/CAB (86/14%) pseudo propellant. As expected  $t_{GE}$ ,  $t_{LE}$ , and  $t_{ign}$  decrease with the increase of incident laser energy flux. The relationship between the  $t_{ign}$  and the incident laser energy flux were correlated and the results are also shown in these figures. The region below the curves represents the no ignition zone and the region above the curves can be regarded as the self-sustained combustion zone. The data for  $t_{GE}$  and  $t_{LE}$  exhibited a considerable degree of scattering at low energy flux of 50 W/cm<sup>2</sup> which could be associated with the heterogeneous foam-layer

behavior and stability of the laser energy output at low levels. When the energy flux is increased,  $t_{GE}$ ,  $t_{LE}$ , and  $t_{ign}$  became closer to each other, and the data scattering was significantly reduced. Based upon the results of ignition tests, it was found that  $t_{ign}$  of pure HMX was 17-40% lower than those of pure RDX. This result is unexpected from the point of view of thermal heating of two different inert materials in the subsurface region.

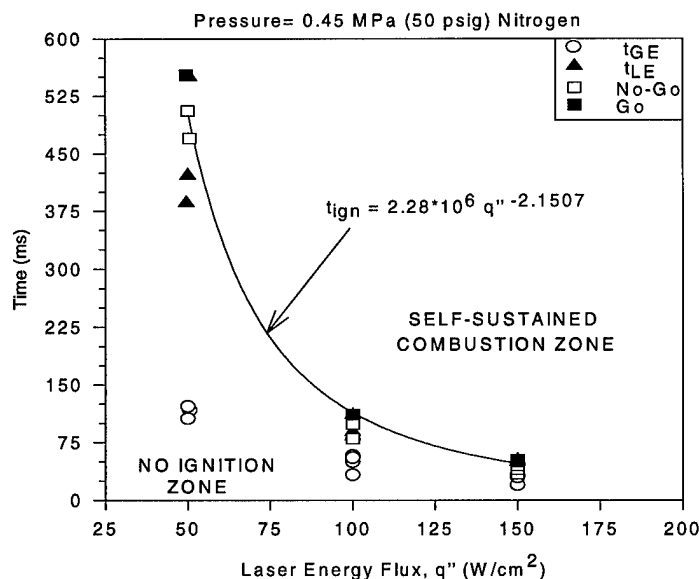


Figure 4.5 Ignition delay times for pure RDX.

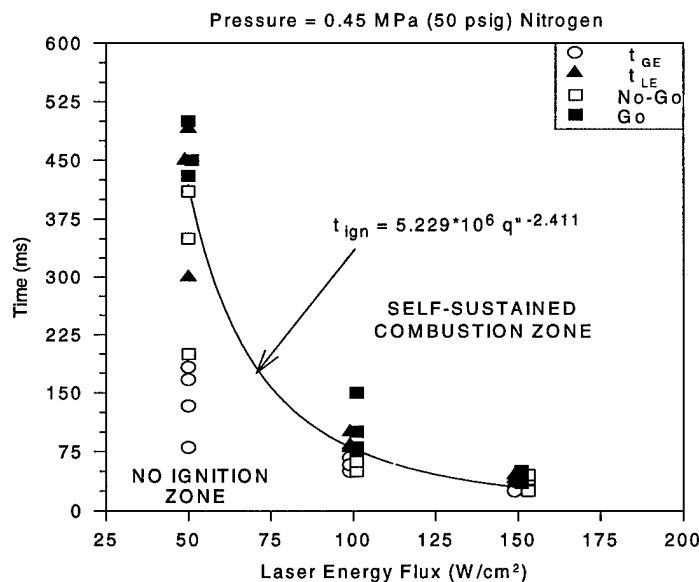


Figure 4.6 Ignition delay times for pure HMX.

The thermal diffusivity,  $\alpha$ , of a propellant is a measure of the energy diffusion rate into the preheat zone beneath the surface. The higher the  $\alpha$ , the deeper the thermal wave penetration. The  $\alpha$  value of HMX is larger than that of RDX which implies that the thickness of the preheat zone for HMX is larger than that of RDX if the subsurface reaction zone is inert. Also the required surface temperature to reach melting is higher for HMX than RDX.

Therefore, it is generally anticipated that HMX requires longer time to reach a critical surface temperature for ignition than RDX. The results obtained by T. P. Parr and D. Hanson-Parr of NAWC also showed that at high laser heating (around  $600 \text{ W/cm}^2$ ), HMX had longer ignition delay times than RDX. The reason for the reversed trend of  $t_{\text{ign}}$  of HMX and RDX in the current study is believed to be due to the existence of a very dynamic two-phase surface region of RDX. At low pressures, RDX has a very thick foam layer ( $\sim 1 \text{ mm}$ ) which consists of many large bubbles. At lower heat fluxes (around  $50$  to  $150 \text{ W/cm}^2$ ), as in the case of current study, the thick and dynamic foam layer of RDX is believed to have some shielding effect which results in a longer  $t_{\text{ign}}$ . At very high heat fluxes, the effect of foam layer shielding diminishes and therefore  $t_{\text{ign}}$  for HMX is longer than those of RDX. From the results of ignition tests, it was also found that the Go/No-Go ignition boundary increases with the increase of CAB content in pseudo propellants except for RDX at low energy fluxes (i.e., around  $50$  and  $100 \text{ W/cm}^2$ ). The reason for the reversed trend of RDX at low heat fluxes is anticipated to be the stronger interactions between the very dynamic foam layer with the incident laser energy flux at lower flux levels, as explained above. When the CAB percentage was increased to  $11\%$ ,  $t_{\text{ign}}$  increased about  $17\%$  with respect to those of RDX/CAB ( $92/8\%$ ). Further increase in CAB content to  $14\%$  increased the  $t_{\text{ign}}$  about  $73\%$  at  $100$  and  $150 \text{ W/cm}^2$  with respect to those of RDX/CAB ( $92/8\%$ ). The increase of  $t_{\text{ign}}$  of pseudo propellants with CAB percentage is due to the higher specific heat of CAB than that of RDX; therefore, CAB absorbs more energy for the same amount of temperature increase, which yields higher values of  $t_{\text{ign}}$ .

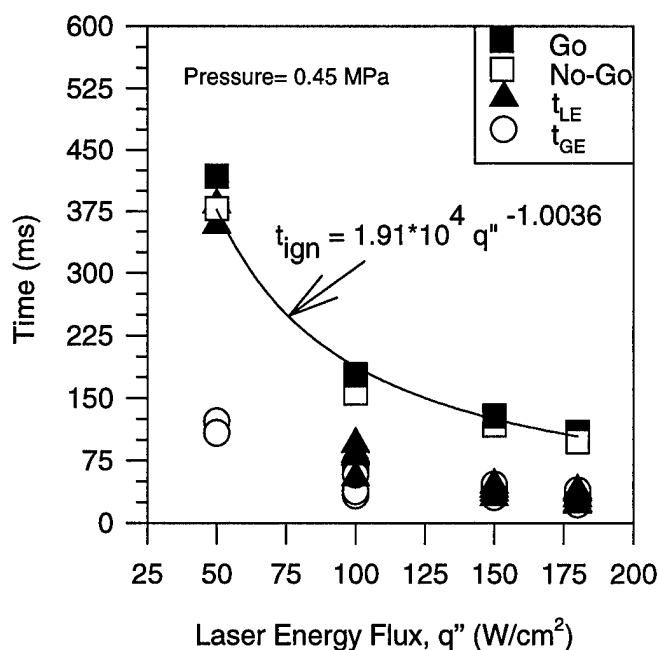


Figure 4.7 Ignition delay times for RDX/CAB (86/14%) pseudo propellant.

It is well known that when the exponent in a simple power-law expression (i.e.,  $t_{\text{ign}} = a [q'']^n$ ) is equal to  $-2$ , it corresponds to the inert heating process prior to ignition. For pure RDX, the exponent is  $-2.151$ , which is very close to  $-2$ ; therefore, the surface of RDX can be regarded as almost inert during the ignition period. When the CAB percentage is increased to  $8\%$ , the

exponent increased to -1.545. This indicates that there are some surface reactions (mostly endothermic) which require a longer time for the laser energy to be transferred to the surface in order to bring the sample to ignition condition. The exponent further increased to -1.497 for RDX/CAB (89/11%) pseudo propellant indicating more endothermic surface reactions. For RDX/CAB (86/14%) pseudo-propellant, the exponent, was -1.004 due to even higher endothermic surface reactions.

The results obtained during this research investigation are believed to be very useful for understanding the combustion behavior of these propellants and for model validation.

#### IV.3 References

- 4.1 Vandeheoff, J. A. and Kotlar, A. J. (1990). Simultaneous Determination of Temperature and OH Concentrations in a Solid Propellant Flame. *Proceedings of the 23<sup>rd</sup> Symposium (International) on Combustion*, pp. 1339-1344.
- 4.2 Hanson-Parr, D. and Parr, T. (1993). RDX Laser-Assisted Flame Structure. *31<sup>st</sup> JANNAF Combustion Meeting*.
- 4.3 Edwards, T., Weaver, D. P., and Campbell, D. H. (1987). Laser-Induced Fluorescence in High Pressure Solid-Propellant Flames. *Applied Optics*, 26, 3496.
- 4.4 Lu, Y. C., A. Ulas, K. K. Kuo, and T. M. Freyman (1995). Absorption Spectroscopy of Solid Propellant Flames. *31<sup>st</sup> AIAA/ASME/SAE/ASEE Joint Propulsion Conference and Exhibit*, AIAA 95-2713, 1995.
- 4.5 Lu, Y. C., T. Freyman, and K. K. Kuo (1995). Measurement of Temperatures and OH Concentrations of Solid Propellant Flames using Absorption Spectroscopy. *Comb. Sci. and Tech.*, Vol. 104, pp. 193-205, 1995.
- 4.6 Ulas, A., Y.C. Lu, T.M. Freyman, and Kuo, K.K., "Measurement of Temperatures and NO and OH Concentrations of Solid Propellant Flames Using Absorption Spectroscopy," *32nd JANNAF Combustion Subcommittee Meeting*, Huntsville, AL, CPIA Publication 631, Volume I, pp. 461-469, October 23-27, 1995.
- 4.7 Lu, Y.-C., T. Freyman, and K.K. Kuo, "Measurement of Temperatures and OH Concentrations of Solid Propellant Flames using Absorption Spectroscopy," *31<sup>st</sup> JANNAF Combustion Subcom. Meeting*, Oct. 17-21, 1994, Sunnyvale, CA, CPIA Public. 620, Vol. II, pp. 277-290.
- 4.8 Ulas, A., Lu, Y.C., Kuo, K.K., and Chang, Y.P., "Ignition Delay and Flame Structure Measurements of RDX-Based Pseudo Propellants," *Proceedings of the 33rd JANNAF Combustion Subcommittee Meeting*, Monterey, CA, CPIA publication 653, Volume II, pp. 391-402, November, 1996.
- 4.9 Lu, Y.-C., A.Ulas, E. Boyer, and K.K. Kuo, "Determination of Temperature Profiles of Self-Deflagrating RDX by UV/Visible Absorption Spectroscopy and Fine-Wire Thermocouples," *Comb. Sci. and Tech.*, Vol. 123, No.1-6, pp. 147-163, 1997.
- 4.10 Ulas, A., Y.C. Lu, and Kuo, K.K., "Determination of Temperature and OH Concentration Profiles of RDX/CAB Pseudo Propellants Using UV/Visible Absorption

Spectroscopy," *Challenges in Propellants and Combustion 100 Years After Nobel*, Begell House, Inc., New York, pp. 885-895, 1997.

- 4.11 Ulas, A., Y.C. Lu, and Kuo, K.K., "Ignition Delay and Flame Structure Measurements of RDX-Based Pseudo Propellants," *Proceedings of the 24<sup>th</sup> International Pyrotechnics Seminar*, pp. 531-542, Monterey, CA, 27-31 July, 1998.

## **V. Thermal Decomposition Studies of Nitramine Propellant Binder Ingredients**

### **V.1 Statement of Problem**

The flash pyrolysis chemistry of the main components of the XM39 LOVA propellant (RDX, NC, and CAB) was characterized by T-jump/FTIR spectroscopy. The objective was to define better the species and rate constants that might be incorporated into a combustion model. In addition, mixtures of RDX/NC and CAB/RDX were characterized for comparison with the pure components.

### **V.2 Summary of Most Important Results**

Although much previous work has been conducted on the decomposition of the cyclic nitramines RDX and HMX, there was a need to compile and analyze previous studies in the context of the more recent work. The kinetic compensation effect in RDX and HMX was analyzed in the slow decomposition range.<sup>5.1</sup> The kinetics and reaction channels of RDX were then analyzed in the temperature range of the burning surface.<sup>5.2</sup> This latter article considered the history of the inclusion of the surface reaction zone models, the use of global surface rates, the use of specific reactions, and the incorporation of vaporization. The "minor" products from flash pyrolysis of RDX were also determined by the use of multivariate regression methods for the first time.<sup>5.3</sup> It was possible to remove from the spectrum the major gaseous products that were discussed extensively in this team's previous work and to uncover the minor products. Hexahydro-1-nitroso-3,5-dinitro-s-triazine, s-triazine, C-hydroxyl-N-methyl-formamide and both RDX aerosol and RDX vapor were observed in the gaseous phase at concentrations of less than 4 percent. This work helps connect the slow decomposition work of Behrens and Bulusu (Sandia Livermore and ARDEC) and the quenched propellant work of Schroeder, et al. (ARL). Compounds of these types are found in varying amounts in all of these experiments.

In addition to obtaining our own flash pyrolysis data on NC, we analyzed the past kinetics literature for the purpose of reconciling the many conflicts.<sup>5.4</sup> The temperature range of 50-500°C was considered. Below 100°C depolymerization, peroxide formation, and hydrolysis can explain the reported kinetics. At 100-200°C, almost all previously reported kinetics are found to fall into two categories by the use of the kinetic compensation effect. These categories are consistent with first-order decomposition and autocatalytic processes. Above 200°C, the kinetics are consistent with a first-order reaction and desorption which together control the rate.

Flash pyrolysis of cellulose acetate butyrate (CAB) was flash pyrolyzed at set temperatures in the 460-600°C range under 1 atm of Ar for the purpose of identifying the gaseous products and measuring the kinetics.<sup>5.5-5.7</sup> Multivariate regression enabled eleven products (CO, CO<sub>2</sub>, acids, esters, ketenes, aldehydes, and CAB oligomers) to be identified. The ketenes are the

most novel products. Arrhenius activation energies in the lower end of the temperature range are most consistent with control by bulk phase decomposition processes. In the higher temperature range, the desorption processes of these products appear to be rate controlling.

To simulate the decomposition of a LOVA propellant, pseudo-propellants composed of two-component mixtures were made and flash pyrolyzed.<sup>5,8,5,9</sup> An intimate mixture of 88:12 w/w of RDX and CAB and a heterogeneous mixture of 90:10 w/w RDX and NC were made. The gaseous products from these mixtures were compared to the weighted sum of the products from the pure components. RDX stabilizes NC but destabilizes CAB in the time-to-exotherm data. The NO<sub>2</sub> liberated by RDX oxidizes CAB based on the product ratios observed. The project concluded before the study of the interactions between LOVA propellant ingredients could be completed. In general, this subject was proving to be quite complicated and would have required much more research time than was available.

### V.3 References

- 5.1 T. B. Brill, P. E. Gongwer, and G. K. Williams, "Thermal Decomposition of Energetic Materials 66. Kinetic Compensation Effects in HMX, RDX, and NTO," *Journal of Physical Chemistry*, vol. 98, (1994) 12242-12247.
- 5.2 T. B. Brill, "Multiphase Chemistry Considerations at the Surface of Burning Nitramine Monopropellants," *Journal of Propulsion and Power*, vol. 11, (1995) 740-751.
- 5.3 P. E. Gongwer and T. B. Brill, "Thermal Decomposition of Energetic Materials 73. The Identity and Temperature Dependence of "Minor" Products from Flash-Heated RDX," *Combustion and Flame*, vol. 115 (1998) 417-423.
- 5.4 T. B. Brill and P. E. Gongwer, "Thermal Decomposition of Energetic Materials 69. Analysis of the Kinetics of Nitrocellulose at 50-500°C," *Propellants, Explosives, Pyrotechnics*, vol. 22 (1997) 38-44.
- 5.5 P. E. Gongwer, H. Arisawa, T. B. Brill, "Kinetics and Products from Flash Pyrolysis of Cellulose Acetate Butyrate (CAB) at 460-600°C," *Propellants, Explosives, Pyrotechnics*, vol. 22 (1997) 38-44.
- 5.6 P. E. Gongwer, H. Arisawa, T. B. Brill, "Kinetics and Products from Flash Pyrolysis of Cellulose Acetate Butyrate (CAB) at 460-600°C," *Combustion and Flame*, vol. 109 (1997) 370-381.
- 5.7 T. B. Brill, H. Arisawa and P. E. Gongwer, "Combustion-like Pyrolysis of Organic Polymers: Species and Kinetic Details from T-Jump/FTIR Spectroscopy," *Proceedings of the 26<sup>th</sup> International Symposium on Combustion*, (1997) 791-798.
- 5.8 T. B. Brill, H. Arisawa and P. E. Gongwer, "Advances in Combustion-like Kinetics and Mechanisms of Polymeric Binders," in *Challenges in Propellants and Combustion 100 Years after Nobel*, K. K. Kuo, Ed. Begell House, Inc., 1997, pp. 3-23.
- 5.9 T. B. Brill, P. E. Gongwer and B. Budenz, "Oxidizer-Binder Interactions from T-Jump/FTIR Flash Pyrolysis," *Proceedings of the 28<sup>th</sup> International Conference of the ICT*, Karlsruhe, Germany, 1997, p. 14-1 to 14-11.

- 5.10 T. B. Brill, P. E. Gongwer and B. Budenz, "Condensed-phase Oxidizer-Binder Chemistry During Flash Pyrolysis," Proceedings of the 34<sup>th</sup> JANNAF Combustion Meeting, CPIA Publication 662, (1997) 447-456.

## **VI. In Situ Observation of Burning Surface Phenomena**

### **VI.1 Statement of Problem**

It is generally known that a complex surface reaction zone exists on the burning surface of nitramine propellants at pressures less than 6.87 MPa (1000 psia). Although this layer is acknowledged to play an important role in the combustion process, its detailed structure remains relatively uncharacterized due to variations with propellant formulation and operating conditions as well as the difficulty of instrumentation under combustion conditions.

### **VI.2 Summary of Most Important Results**

Near surface burning phenomena were investigated for 0.64 cm (0.25 in) diameter samples of pure RDX, nitramine-based composite propellants M43 and XM39, and JA-2 a modified double-base homogeneous propellant over a pressure range of 0.10 to 3.55 MPa. The RDX test samples were consolidated from recrystallized powder into cylindrical pellets 0.64 cm in diameter and approximately 0.70 cm long in a specially designed presser system. The other propellants were cut from 0.64 cm strands into samples approximately 1.27 cm long. A Pulnix color CCD camera equipped with a 60-mm micro lens provided high-magnification images which were recorded on a Panasonic S-VHS VCR to produce high-quality video for post-test analysis and image processing. To allow observation of the burning surfaces over a range of pressures, a windowed test chamber pressurized with nitrogen gas was used. A constant flow of nitrogen purge gas past the sample kept the chamber clear of smoke and ensured a relatively flat burning surface. The samples were ignited by a 50-W CO<sub>2</sub> laser projected on the top surface of the propellant until a steady burn was achieved.<sup>6,1</sup>

At low pressures, such as 0.17 MPa (10 psig), RDX pellets exhibited a thick, bubbly layer as shown in Fig. 6.1. The foam layer was thickest at the center (about 400  $\mu$ m) and tapered to the edges of the sample due to surface tension and edge cooling effects. A distinct dark zone of about 100  $\mu$ m was also present. At 1 atm, the foam zone thickness was about 650  $\mu$ m at the center and the dark zone was about 450  $\mu$ m thick. Dark zone size, foam layer thickness, and bubble size decreased as pressure increased. The dark zone was no longer visible at 0.44 MPa (50 psig) as the luminous flame began to attach to the surface. Carbonaceous patches at the point of attachment are believed to form hot spots enhancing heat transfer and radical generation at these locations. Although bubbles were not visible above 0.93 MPa (120 psig), a liquid layer was observed on the surface at all conditions tested, up to 2.23 MPa (310 psig).

Behavior of M43 and XM39 propellants appeared much the same due to similarity of these two formulations. Small mobile carbonaceous particles in the liquid layer agglomerated into flame-holding sites at higher pressures for both propellants. Figure 6.2 shows the flame attached to agglomerates on the surface of M43 at 1.23 MPa (165 psig). The pressure at which the liquid layer disappeared for M43 (185 psig) was lower than that for XM39 (>500 psig). This is believed to be caused by the higher heat release in the surface reaction zone of M43 which contains a more energetic plasticizer than the ATEC in XM39.

Large carbonaceous flakes formed on the burning surface of JA-2 were observed at all pressures. No flame was visible at pressures below 1.23 MPa (165 psig) due to fizz burning. At 1.48 MPa (200 psig), the carbonaceous flakes acted as flame holders as shown in Fig. 6.3 with the number of attachment sites increasing with pressure. At higher pressures (e.g. 500 psig), nearly uniform flame attachment to a glowing structure on the surface was observed. No liquid layer was observed at any test condition.

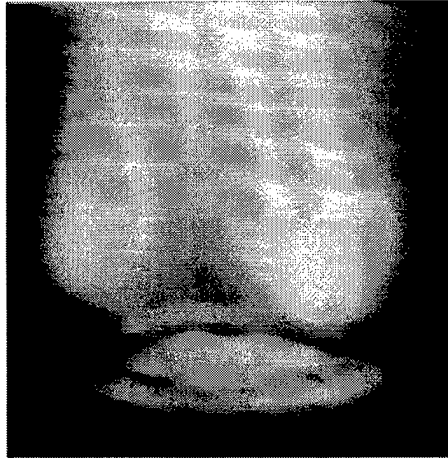


Figure 6.1 Thick foam layer on burning surface of RDX at 0.17 MPa (10 psig).

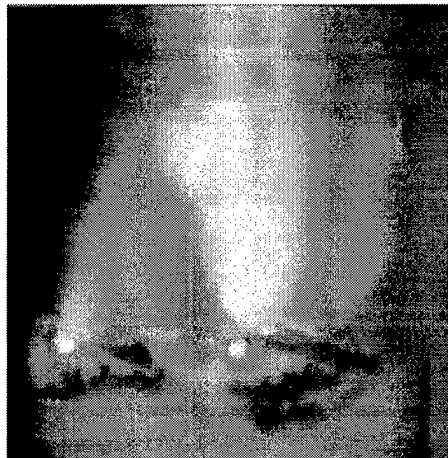


Figure 6.2 Flame attachment to agglomerates on M43 at 1.23 MPa (165 psig).

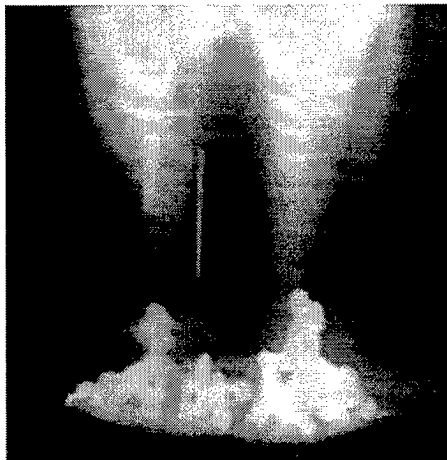


Figure 6.3 Flame attachment to carbonaceous flakes on JA-2 at 1.48 MPa (200 psig).

Many different samples of RDX-based propellant and propellant ingredients have been imaged using a hot-stage equipped Environmental Scanning Electron Microscope (ESEM) while undergoing heating. When heated over a temperature range of 25°C to 450°C, XM39 propellant showed very interesting behavior. Around 170 °C, well below the melting point of RDX, the propellant structure began to change and a liquefaction process was observed at ~180°C. Many bubbles were observed developing between 200 °C and 360 °C as the sample size decreased continuously. As the temperature increased to 450 °C, only a char layer was left. The bubble formation is indicative of liquid-phase vaporization and decomposition, demonstrating that two-phase phenomena are present near the pyrolyzing surface of the sample.

### VI.3 References

- 6.1 Boyer, E., Lu, Y.C., Desmarais, K., and Kuo, K.K., "Observation and Characterization of Burning Surface Reacting Zones of Solid Propellants," 31st JANNAF Combustion Meeting, Sunnyvale, CA, CPIA Publication 620, Vol. II, pp. 211-220, October 17-21, 1994.

## VII. Reactions of RDX and Nitramine-based Propellants

### VII.1 Statement of Problem

Since the regression rate of solid propellants can be greatly influenced by surface and subsurface reactions, better knowledge of condensed phase reactions is vital to gain a more in-depth understanding of the combustion of nitramine solid propellants. Surface and near-surface phenomena of RDX-based propellants have not been fully studied, mainly due to the difficulties in probing the thin surface reaction zone. Any intrusive probing of the reaction zone (which has a relatively small characteristic length on the order of 100  $\mu\text{m}$ ) could significantly disturb the localized combustion phenomena. Many previous studies have focused on experiments at non-combustion conditions to investigate thermal decomposition rates and reaction mechanisms of solid propellants and their ingredients.

### VII.2 Summary of Most Important Results

A microprobe mass spectrometer was used to measure decomposition products from the subsurface region of XM39 and M43 RDX-based propellants. The microprobe was inserted

into a hole drilled axially in the centerline of each propellant sample. Gaseous species released in the subsurface region were collected in the cavity and were sucked into the probe and analyzed.<sup>7.1</sup> Tests were conducted in Ar at 1 and 3 atm, with a CO<sub>2</sub> laser external heat flux of 100, 200, and 275 W/cm<sup>2</sup>. An insignificant amount of solid-phase decomposition products was detected for M43, and only a very minute amount of oxy-s-triazine (OST) was detected from XM39 at very low heat flux conditions. At the time of burn through, the major species detected had masses of 30, 28, 44, and 27 amu, believed to be CH<sub>2</sub>O, CO, N<sub>2</sub>O, and HCN.<sup>7.2,7.3</sup> These products suggest that the RDX decomposition pathway to form CH<sub>2</sub>O and N<sub>2</sub>O is more dominant for the condensed-phase reactions at the operating conditions studied. The cellulose acetate butyrate (CAB) binder and plasticizers of these two propellants showed relatively inactive behavior under the conditions tested.

### VII.3 References

- 7.1 Boyer, E., Y.C. Lu, and K.K. Kuo, "Characterization of Condensed-Phase Chemical Reactions of RDX," Paper No. AIAA-95-2994, 31st AIAA/ASME/SAE/ASEE Joint Propulsion Conference and Exhibit, San Diego, CA, July 10-12, 1995.
- 7.2 Boyer, E., Y.C. Lu, P.W. Brown, and K.K. Kuo, "The Characterization of the Burning Surface of Nitramine Propellants," 32nd JANNAF Combustion Subcommittee Meeting, Huntsville, AL, CPIA publication 631, October 23-27, 1995.
- 7.3 Boyer, E., Y.C. Lu, and K.K. Kuo, "Characterization of Condensed-Phase Chemical Reactions of RDX and Nitramine-Based Propellants," *Challenges in Propellants and Combustion 100 Years After Nobel*, Begell House, Inc., New York, pp. 906-917, 1997.

## VIII. Condensed-phase Interactions between RDX and Common Solid Propellant Binders

### VIII.1 Statement of Problem

In comparison to the studies of decomposition and subsequent reactions involving RDX and other propellant ingredients, very little attention has been given to the effects of solid-state interactions in the condensed phase. The combination of ingredients in solid propellants (e.g., oxidizer, binders, plasticizers, etc.) may not be adequately modeled as just a physical mixture. This is due to the fact that some interactions between these components can change intermolecular forces in the propellant mixture, leading to changes in physical properties and combustion behavior. If there is appreciable solid solubility, solutions will form and will have enthalpies of fusion, melting temperatures, and other characteristics different from those of pure substances. It is desirable to establish the properties of such mixtures when designing new propellant formulations.

### VIII.2 Summary of Most Important Results

The solubilities of common propellant ingredients including acetyl triethyl citrate (ATEC), cellulose acetate butyrate (CAB), nitrocellulose (NC), and the energetic plasticizer (EP) used in M43 propellant and their effects on RDX unit cell dimensions were investigated. Samples were aged at an elevated temperature to speed the formation of solid solutions. A least-squares analysis of X-ray diffraction data was used to obtain the lattice parameters from which unit cell volume and solubility were deduced.<sup>8.1</sup> X-ray powder diffraction analysis showed that all binders tested formed a solid solution with RDX indicated by expansion of the RDX unit cell volume. CAB was found to have a solubility limit greater than 16 wt%,

while EP had the least. NC and ATEC both showed solubility up to about the 9 wt% level. Changes in material and combustion properties due to the solid solution formation should therefore be closely examined in the modeling of combustion processes of RDX-based composite propellants.<sup>8,2</sup>

### VIII.3 References

- 8.1 Boyer, E., P.W. Brown, and K.K. Kuo, "Phase Relationships Involving RDX and Common Solid Propellant Binders," *Decomposition, Combustion, and Detonation Chemistry of Energetic Materials*, Vol. 418, T.B. Brill, et al. (Editors), Materials Research Society, Pittsburgh, PA, pp. 79-84, 1995.
- 8.2 Boyer, E., P.W. Brown, and K.K. Kuo, "Solid Solution Formation between RDX and Common Solid Propellant Binders," *Challenges in Propellants and Combustion 100 Years After Nobel*, Begell House, Inc., New York, pp. 387-394, 1997.

## IX. Effects of Processing Procedures on Pseudo-Propellant Flame Structure

### IX.1 Statement of Problem

Understanding the formation and influencing factors on the dark zone above RDX-based propellants is essential in the formulation of accurate models for combustion simulation.

### IX.2 Summary of Most Important Results

Combustion behavior and flame zone structure of various RDX-based pseudo-propellants were compared to neat RDX and actual XM39 propellant. It was found that the existence of a dark zone over the pseudo-propellant samples was dependent on the processing procedure used. None of the shock-precipitated and pressed samples showed a dark zone at any test condition. However, an extrusion process utilizing ethyl acetate solvent produced pseudo-XM39 that duplicated the combustion behavior and flame structure of actual XM39 at the reference test conditions of 150 psig and 300 psig in an N<sub>2</sub> atmosphere. RDX/CAB (80/20 wt%) pseudo-propellant also showed a dark zone of approximately 4 mm at 300 psig.<sup>9,1,9,2</sup> As shown by other researchers, the addition of binders to RDX is a necessary condition in the formation of a dark zone over the burning surface. However, it is seen here not to be a sufficient condition, as all pressed pseudo-propellant mixtures showed flame attachment without dark zones. It is believed that the microstructure of propellant is an important factor in dark zone formation. With the CAB binder matrix wetting and surrounding RDX particles in extruded samples, dark zones were observed.

### IX.3 References

- 9.1 Boyer, E. and Kuo, K.K., "Effects of Processing Procedures and Propellant Ingredients on the Presence of Dark Zone of RDX-Based Pseudo-Propellants," Proceedings of the 33rd JANNAF Combustion Subcommittee Meeting, Monterey, CA, CPIA publication 653, Volume II, pp. 579-587, November, 1996.
- 9.2 Boyer, E., and K.K. Kuo, "Influence of Processing Procedures and Propellant Ingredients on RDX-Based Pseudo-Propellant Dark Zone," AIAA Paper No. 97-3235, 33rd AIAA/ASME/SAE/ASEE Joint Propulsion Conference, Seattle, WA, July 6-9, 1997.

## X. Nitromethane Combustion

### X.1 Statement of Problem

Nitromethane has been considered to have some burning features similar to the solid RDX while having a simpler molecular structure. It is believed that knowledge of the nitromethane flame structure and burning behavior will further enhance the understanding of the ignition and combustion of nitramines (such as RDX and HMX) and other nitro group-containing materials and compounds.

### X.2 Summary of Most Important Results

The intrinsic burning rate of nitromethane over a range of pressures and initial temperatures was measured using an optically accessible, high-pressure liquid propellant strand burner (LPSB) established at PSU. Compared to other methods, the LPSB minimizes undesirable effects introduced by gelling agents and LP-containing tubes that may modify burning behavior. To determine the intrinsic burning rate, chamber pressure was varied to achieve a steady-state level of the LP burning surface at a set actuator feeding rate.<sup>10.1</sup> Burning rates at four different initial temperatures from -30 °C to +45 °C were determined in an air environment. Over a pressure range of 2.5 to 15 MPa (250 to 2200 psig), the intrinsic burning rate of nitromethane was determined as a power law of chamber pressure for the four different initial temperatures. Data and a power-law curve fit for each temperature are shown in Fig. 10.1. Temperature sensitivity ( $\sigma_p$ ) was then deduced and found to be most sensitive to initial temperature change at low pressures, with the temperature sensitivity  $\sigma_p = 2.9 \times 10^{-3} \text{ K}^{-1}$  at 2.51 MPa (350 psig). The  $\sigma_p$  decreases greatly with increasing pressure, dropping to a very low value of  $0.6 \times 10^{-3} \text{ K}^{-1}$  at a pressure of 9.96 MPa (1430 psig). A second-order polynomial<sup>10.2</sup> fits the deduced points very well:  $\sigma_p = 4.38 \times 10^{-3} - 6.73 \times 10^{-4}P + 2.97 \times 10^{-5}P^2$  where  $P$  is in MPa and  $\sigma_p$  in  $\text{K}^{-1}$ . The trend indicates even less sensitivity at higher pressures. The tube confinement encountered in conventional LP burning-rate measurements proved to have a non-negligible effect in reduction of the LP burning rate. This indicates that the advantage of using the LPSB for determining the intrinsic burning rates of liquid propellants.

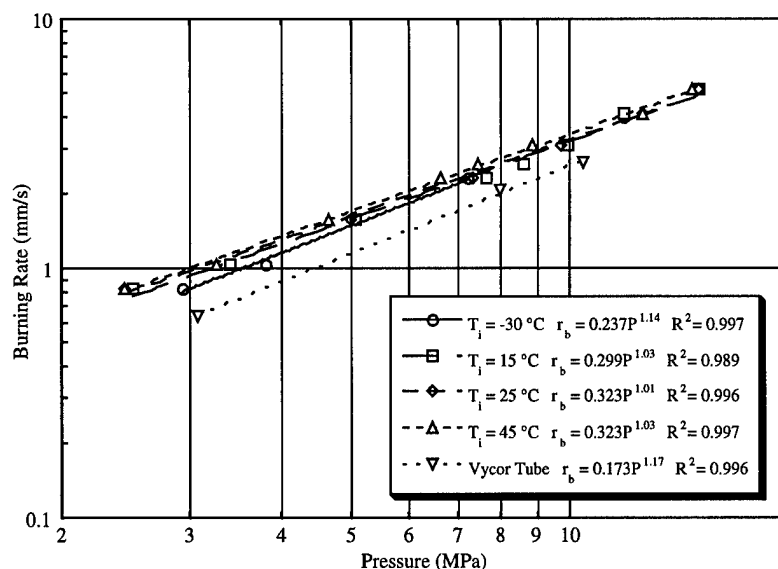


Figure 10.1 Burning rate of nitromethane at different pressures and initial temperatures.

### X.3 References

- 10.1 Lu, Y.C., E. Boyer, D. Koch, and K.K. Kuo, "Measurement of Intrinsic Burning Rate of Nitromethane," AIAA Paper No. 97-3107, 33rd AIAA/ASME/SAE/ASEE Joint Propulsion Conference, Seattle, WA, July 6-9, 1997.
- 10.2 Boyer, E., D. Koch, K.K. Kuo, and Y.C. Lu, "Intrinsic Burning Rate and Temperature Sensitivity of Nitromethane," Proceedings of the 34th JANNAF Combustion Subcommittee Meeting, West Palm Beach, FL, CPIA Publication 662, Volume I, pp. 335-346, October, 1997.

### C. LIST OF PUBLICATIONS AND TECHNICAL REPORTS

- Lu, Y.C., T.M. Freyman, A. Ulas, and K.K. Kuo, "UV/Visible Absorption Spectroscopy of Dark Zones in Solid Propellant Flames," *Combustion and Flame*, Vol. 109, No. 3, pp. 342-352, 1997.
- Wilson, S.J., P.W. Brown, D.K. Smith, and K.K. Kuo, "X-ray Diffraction Studies of RDX," *Powder Diffraction*, (accepted).
- Ulas, A., Y.C. Lu, and K.K. Kuo, "Determination of Temperature and OH Concentration Profiles of RDX/CAB Pseudo-Propellant Using UV/Visible Absorption Spectroscopy," *Challenges in Propellants and Combustion 100 Years After Nobel*, edited by K.K. Kuo, et al., Begell House, Inc.: New York, 1997, pp. 885-895.
- Boyer, E., D. Koch, K.K. Kuo, and Y.C. Lu, "Intrinsic Burning Rate and Temperature Sensitivity of Nitromethane," Proceedings of the 34th JANNAF Combustion Subcommittee Meeting, West Palm Beach, FL, CPIA Publication 662, Volume I, pp. 335-346, October, 1997.
- Boyer, E., Y.C. Lu, and K.K. Kuo, "Characterization of Condensed-Phase Chemical Reactions of RDX and Nitramine-based Propellants," *Challenges in Propellants and Combustion 100 Years After Nobel*, ed. by K.K. Kuo, et al., Begell House, Inc.: New York, 1997, pp. 906-917.
- Boyer, E., P.W. Brown, and K.K. Kuo, "Solid Solution Formation between RDX and Common Solid Propellant Binders," *Challenges in Propellants and Combustion 100 Years After Nobel*, edited by K.K. Kuo, et al., Begell House, Inc.: New York, 1997, pp. 387-394.
- Kuo, K.K., Y.C. Lu, and Y.S. Tseng, "Modeling and Numerical Simulation of Physicochemical Processes Occurring in the Two-Phase Foam Layer of Burning RDX," *Challenges in Propellants and Combustion 100 Years After Nobel*, edited by K.K. Kuo, et al., Begell House, Inc.: New York, 1997, pp. 1133-1145.
- Lu, Y.C., E. Boyer, D. Koch, and K.K. Kuo, "Measurement of Intrinsic Burning Rate of Nitromethane," AIAA Paper 97-3107, presented at 33rd AIAA/ASME/SAE/ASEE Joint Propulsion Conference, Seattle, WA, July 6-9, 1997.
- Boyer, E., and K. K. Kuo, "Influence of Processing Procedures and Propellant Ingredients on RDX-Based Pseudopropellant Dark Zone," AIAA Paper 97-3235, presented at 33rd AIAA/ASME/SAE/ASEE Joint Propulsion Conference, Seattle, WA, July 6-9, 1997.
- Boyer, E., and K.K. Kuo, "Effects of Processing Procedures and Propellant Ingredients on the Presence of Dark Zone of RDX-based Pseudo-Propellants," CPIA Publication 653, Vol. 2, pp. 579-587, 1996; 33rd JANNAF Combustion Subcommittee Meeting, Naval Postgraduate School, Monterey, CA, November 4-8, 1996.

- Ulas, A., Y.C. Lu, K.K. Kuo, and Y.P. Chang, "Ignition Delay and Flame Structure Measurements of RDX-Based Pseudo Propellants," CPIA Publication 653, Vol. 2, pp. 391-402, 1996; 33rd JANNAF Combustion Subcommittee Meeting, Naval Postgraduate School, Monterey, CA, November 4-8, 1996.
- Koch, D., Y.C. Lu, K.K. Kuo, and E. Jones, "Design and Development of a Liquid-Propellant Strand Burner with Initial Application to Nitromethane," CPIA Publication 653, Vol. 1, pp. 127-135, 1996; 33rd JANNAF Combustion Subcommittee Meeting, Naval Postgraduate School, Monterey, CA, November 4-8, 1996.
- Kuo, K.K., "Summary of Fourth ISICP Symposium on Challenges in Propellants and Combustion 100 Years after Nobel," CPIA Publ. 653, Vol. 2, pp. 273-283, 1996; 33rd JANNAF Comb. Subcommittee Meeting, Naval Postgraduate School, Monterey, CA, Nov. 4-8, 1996.
- Boyer, E., P.W. Brown, and K.K. Kuo, "Phase Relationships Involving RDX and Common Solid Propellant Binders," in *Decomposition, Combustion, and Detonation Chemistry of Energetic Materials*, T. B. Brill, T. P. Russell, W. C. Tao, and R. B. Wardle, Eds., Materials Research Society, Symposium Proceedings, Vol. 418, Pittsburgh, PA, pp. 79-84, 1995.
- Ulas, A., Y.-C. Lu, K.K. Kuo, and T. Freyman, "Measurement of Temperatures and NO and OH Concentrations of Solid Propellant Flames Using Absorption Spectroscopy", Proceedings of 32nd JANNAF Combustion Subcommittee Meeting, NASA Marshall Space Flight Center, Huntsville, AL, October 23-27, 1995. CPIA Publication 631, Vol. I, pp. 461-469, Oct., 1995.
- Boyer, E., Y.-C. Lu, and K.K. Kuo, "Characterization of Condensed-Phase Chemical Reactions of RDX and Nitramine-Based Propellants," Proceedings of the 32nd JANNAF Combustion Subcommittee Meeting, NASA Marshall Space Flight Center, Huntsville, Alabama, October 23-27, 1995. CPIA Publication 638, Vol. I, pp. 173-183, October, 1995.
- Laxton, J.A., K.K. Kuo, and Y.C. Lu, "Modeling and Numerical Simulation of Physicochemical Processes Occurring in the Two-Phase Foam Layer of Burning RDX," Proceedings of the 32nd JANNAF Combustion Subcommittee Meeting, NASA Marshall Space Flight Center, Huntsville, AL, October 23-27, 1995. CPIA Publ. 638, Vol. I, pp. 95-106, October, 1995.
- Lu, Y.C., T.M. Freyman, and K.K. Kuo, "Measurement of Temperatures and OH Concentrations of Solid Propellant Flames Using Absorption Spectroscopy," *Combustion Science and Technology*, Vol. 104, No. 1-3, pp. 193-205, 1995.
- Boyer, E., Y.C. Lu, and K.K. Kuo, "Characterization of Condensed-Phase Chemical Reactions of RDX-based Propellants," AIAA Paper 95-2994, 31st AIAA/ASME/SAE/ASEE Joint Propulsion Conference and Exhibit, July 10-12, 1995, San Diego, CA.
- Lu, Y.-C., A. Ulas, and K.K. Kuo, "Absorption Spectroscopy of Solid Propellant Flames," presented at the 1995 Fall Meeting, Materials Research Society, 1995.
- Lu, Y.-C., A. Ulas, K.K. Kuo, and T.M. Freyman, "Absorption Spectroscopy of Solid Propellant Flames," AIAA Paper 95-2713, 31st AIAA/ASME/SAE/ASEE Joint Propulsion Conference and Exhibit, July 10-12, 1995, San Diego, CA.
- Kuo, K.K., and Y.-C. Lu, "Modeling of Physicochemical Processes of RDX Monopropellant with Detailed Treatments for Surface Reaction Zone," *Proceedings of the Twentieth International Pyrotechnics Seminar*, 25-29 July, 1994, Colorado Springs, CO, pp. 583-600.

- Boyer, E., Y.C. Lu, P.W. Brown, and K.K. Kuo, "The Characterization of the Burning Surface of Nitramine Propellants," 32nd JANNAF Combustion Subcommittee Meeting, Huntsville, AL, CPIA publication 631, October 23-27, 1995.
- Boyer, E., Y.-C. Lu, K. Desmarais, and K.K. Kuo, "Observation and Characterization of Burning Surface Reaction Zones of Solid Propellants," 31st JANNAF Combustion Subcommittee Meeting, October 17-21, 1994, Sunnyvale, CA, CPIA Public. 620, Vol. II, pp. 211-220.
- Lu, Y.-C., T.M. Freyman, and K.K. Kuo, "Measurement of Temperatures and OH Concentrations of Solid Propellant Flames Using Absorption Spectroscopy," 31st JANNAF Combustion Subcom. Meeting, Oct. 17-21, 1994, Sunnyvale, CA, CPIA Public. 620, Vol. II, pp. 277-290.
- Lu, Y.-C., T. M. Freyman, G. Hernandez, and K. K. Kuo, "Measurement of Temperatures and Radical Concentrations of Solid Propellant Flames Using Absorption Spectroscopy," Fall Technical Meeting 1994, Eastern States Section: The Combustion Institute, Clearwater Beach, FL, December 5-7, 1994.
- Lu, Y.-C., T.M. Freyman, G. Hernandez, and K.K. Kuo, "Measurement of Temperatures and OH Concentrations of Solid Propellant Flames Using Absorption Spectroscopy," AIAA Paper 94-3040, presented at the 30th AIAA/ASME/SAE/ASEE Joint Propulsion Conference, Indianapolis, Indiana, June 27-30, 1994.
- Kuo, K.K., T. A. Litzinger and W.H. Hsieh, "Interrelationship Between Solid Propellant Combustion and Materials Behavior," invited paper published in Symposium Proceedings on Structure and Properties of Energetic Materials, Vol. 296, pp. 331-348, 1993.
- Kuo, K.K., and Y.-C. Lu, "Modeling of Physicochemical Processes of Burning RDX Monopropellants," CPIA Publ. 606, Vol. II, 1993 JANNAF Combustion Subcommittee Meeting, Monterey, CA, pp. 235-257, November, 1993.
- Wilson, S.J., B.L. Fetherolf, P.W. Brown, and K. K. Kuo, "Surface Microstructure Resulting from Laser-Induced Pyrolysis and Combustion of M43 and XM39," CPIA Publ. 606, Vol. II, 1993 JANNAF Comb. Subcommittee Meeting, Monterey, CA, pp. 167-182, Nov., 1993.
- Fetherolf, B.L., Y.-C. Lu, T.A. Litzinger, and K.K. Kuo, "A Comparison of the Physical and Chemical Processes Governing the CO<sub>2</sub> Laser-Induced Deflagration of XM39 and M43," CPIA Publ. 606, Vol. II, 1993 JANNAF Combustion Subcommittee Meeting, Monterey, CA, pp. 183-193, November, 1993.
- Kuo, K.K., and Y.-C. Lu, "Modeling of Physicochemical Processes of Burning RDX Monopropellants," invited paper, presented and accepted for publication in the Proceedings of the 1993 International Conference on Combustion, Moscow, June 1993, 34 pages.
- Mallery, C.F., and S.T. Thynell, "Line-of-Sight Profiling of Temperature and Species in Propellant Flames Using FTIR Spectroscopy," Proceedings of the 34th JANNAF Combustion Subcommittee Meeting, West Palm Beach, Florida, October 27-31, 1997; also AIAA Paper 98-3827, presented at the 34th AIAA/ASME/SAE/ASEE Joint Propulsion Conference and Exhibit, July 12-15, 1998, Cleveland, OH.
- Kim, E.S., and Thynell, S.T., "Condensed-Phase Kinetic Rates of RDX from Confined Rapid Thermolysis/FTIR Spectroscopy," AIAA Paper No. 98-3828 presented at the 34<sup>th</sup> AIAA/ASME/SAE/ASEE Joint Propulsion Conference and Exhibit, Cleveland, OH, July 13-15, 1998.

- Ulas, A., Y.C. Lu, and Kuo, K.K., "Ignition Delay and Flame Structure Measurements of RDX-Based Pseudo Propellants," *Proceedings of the 24<sup>th</sup> International Pyrotechnics Seminar*, pp. 531-542, Monterey, CA, 27-31 July, 1998.
- Mallery, C.F., and S.T. Thynell, "Species and Temperature Profiles of Propellant Flames Obtained from FTIR Absorption Spectrometry," *Combustion Science and Technology*, Vol. 122, pp. 113-129, 1997.
- Kim, E.S., H.S. Lee, C.F. Mallery, and S.T. Thynell, "Thermal Decomposition Study of Energetic Materials Using Confined Rapid Thermolysis/FTIR Spectroscopy," *Combustion and Flame*, Vol. 110, pp. 239-255, 1997.
- Mallery, C.F., and S.T. Thynell, "Line-of-Sight Temperature and Species Profiles Determined from Spectral Transmittances," *J. Thermophysics and Heat Transfer*, Vol. 11, No. 3, pp.367-374, 1997.
- Lu, Y.-C., A.Ulas, E. Boyer, and K.K. Kuo, "Determination of Temperature Profiles of Self-Deflagrating RDX by UV/Visible Absorption Spectroscopy and Fine-Wire Thermocouples," *Comb. Sci. and Tech.*, Vol. 123, No.1-6, pp. 147-163, 1997.
- Thynell, S.T., T.B. Brill, and P. Gongwer, "Condensed-Phase Kinetics of Cyclotrimethylenetrinitramine by Modeling the T-jump/Infrared Spectroscopy Experiment," *Journal of Propulsion and Power*, Vol. 12, No. 5, pp. 933-939, 1996.
- Litzinger, T.A., Y. Lee, C-J. Tang, and G. Kudva, "The Near-Surface Gas-Phase Structure of RDX During CO<sub>2</sub> Laser-Assisted Combustion," 32<sup>nd</sup> JANNAF Combustion Subcommittee Meeting, Huntsville, AL, October 1995.
- Mallery, C.F., E. Kim, and S.T. Thynell, "High-pressure Strand Burner System for Propellant Flame Studies Using Absorption Spectroscopy," *Review of Scientific Instruments*, Vol. 66, No. 8, pp. 4091-4094, 1995.
- Mallery, C.F., and S.T. Thynell, "Further Improvements to FTIR Absorption Spectroscopy of Propellant Flames for Profiling of Species and Temperature," Proceedings of the 32nd JANNAF Combustion Subcommittee Meeting, NASA Marshall Space Flight Center, Huntsville, Alabama, October 23-27, 1995. CPIA Publication 631, Vol. I, pp. 449-460, October, 1995.
- Mallery, C.F., and S.T. Thynell, "Radial Temperature and Species Profiles from an Inverse Analysis of Spectral Transmittances," AIAA-paper 97-0120 presented at the 35th Aerospace Sciences Meeting, Reno, Nevada, (January 8-11, 1997); CPIA Publication 653, Vol. 2, pp. 371-382, 1996; presented at the 1996 JANNAF Combustion Subcommittee Meeting, Naval Postgraduate School, Monterey, CA, November 4-8, 1996.
- Mallery, C.F., and S.T. Thynell, "Species and Temperature Profiles of Propellant Flames Obtained from FTIR Absorption Spectrometry," 31st JANNAF Combustion Subcommittee Meeting, October 17-21, 1994, Sunnyvale, CA, CPIA Publication 620, Vol. II, pp. 291-305.
- Thynell, S.T., T.B. Brill, and P. Gongwer, "Modeling of Thermal Response of Filament Used in T-jump Experiment," 31st JANNAF Combustion Subcommittee Meeting, October 17-21, 1994, Sunnyvale, CA, CPIA Publication 620, Vol. II, pp. 221-232.
- Thynell, S.T., C.F. Mallery, and E. Kim, "FT-IR Absorption Spectrometry of Propellant Flames," Proceedings of the 30<sup>th</sup> JANNAF Subcommittee Combustion Meeting, Naval Postgraduate

- School, Monterey, CA, November 15-19, 1993; CPIA Publication 606, Vol. II, pp. 307-318, 1993.
- Gongwer, P.E., and T. B. Brill, "Thermal Decomposition of Energetic Materials 73. The Identity and Temperature Dependence of "Minor" Products from Flash-Heated RDX," *Combustion and Flame*, vol. 115 (1998) 417-423.
- Brill, T.B., and P. E. Gongwer, "Thermal Decomposition of Energetic Materials 69. Analysis of the Kinetics of Nitrocellulose at 50-500°C," *Propellants, Explosives, Pyrotechnics*, vol. 22 (1997) 38-44.
- Gongwer, P.E., H. Arisawa, and T. B. Brill "Kinetics and Products from Flash Pyrolysis of Cellulose Acetate Butyrate (CAB) at 460-600°C," *Propellants, Explosives, Pyrotechnics*, vol. 22 (1997) 38-44.
- Gongwer, P.E., H. Arisawa, and T. B. Brill "Kinetics and Products from Flash Pyrolysis of Cellulose Acetate Butyrate (CAB) at 460-600°C," *Combustion and Flame*, vol. 109 (1997) 370-381.
- Brill, T.B., H. Arisawa, and P. E. Gongwer, "Combustion-like Pyrolysis of Organic Polymers: Species and Kinetic Details from T-Jump/FTIR Spectroscopy," *Proceedings of the 26<sup>th</sup> International Symposium on Combustion*, (1997) 791-798.
- Brill, T.B., H. Arisawa, and P. E. Gongwer, "Advances in Combustion-like Kinetics and Mechanisms of Polymeric Binders," in *Challenges in Propellants and Combustion 100 Years after Nobel*, K. K. Kuo, Ed., Begell House, Inc., 1997, pp. 3-23.
- Brill, T.B., P. E. Gongwer, and B. Budenz, "Oxidizer-Binder Interactions from T-Jump/FTIR Flash Pyrolysis," *Proceedings of the 28<sup>th</sup> International Conference of the ICT*, Karlsruhe, Germany, 1997, p. 14-1 to 14-11.
- Brill, T.B., P. E. Gongwer, and B. Budenz, "Condensed-phase Oxidizer-Binder Chemistry During Flash Pyrolysis," *Proceedings of the 34<sup>th</sup> JANNAF Combustion Meeting*, CPIA Publ., 662, (1997) 447-456.
- Gongwer, P.E., H. Arisawa, and T. B. Brill, "Products and Kinetics of Flash Pyrolysis of Cellulose Acetate Butyrate: The Binder of LOVA," *Materials Research Society*, vol. 418, (1996) p. 233-238.
- Brill, T.B., H. Arisawa, P. J. Brush, P. E. Gongwer, and G. K. Williams, "Surface Chemistry of Burning Explosives and Propellants," *Journal of Physical Chemistry*, vol. 99 (1995) p. 1384-1392.
- Brill, T.B., "Multiphase Chemistry Considerations at the Surface of Burning Nitramine Monopropellants," *Journal of Propulsion and Power*, vol. 11, (1995) 740-751.
- T. B. Brill, P. E. Gongwer, and G. K. Williams, "Thermal Decomposition of Energetic Materials 66. Kinetic Compensation Effects in HMX, RDX, and NTO," *Journal of Physical Chemistry*, vol. 98, (1994) 12242-12247.
- Brill, T.B., P. E. Gongwer, and G. K. Williams "Thermal Decomposition of Energetic Materials 66. Kinetic Compensation Effects in HMX, RDX, and NTO," *Journal of Physical Chemistry*, vol. 98, (1994) 12242-12247.

- Kudva, G., C.-J. Tang, Y.-J. Lee, and T.A. Litzinger, "Study of Laser-Assisted Combustion of Nitramine Propellants," presented at the Eastern States Section of the Combustion Institute, 1996 Fall Technical Meeting, Hilton Head, SC, December, 1996.
- Kudva, G., C.-J. Tang, Y.-J. Lee, and T.A. Litzinger, "Study of Laser-Assisted Combustion of RDX-CAB Pseudo-Propellants at Various Operating Conditions," CPIA Publication 653, Vol. 2, pp. 569-578, 1996; 33rd JANNAF Subcommittee Meeting, Naval Postgraduate School, Monterey, CA, November 4-8, 1996.
- Kudva, G., C.-J. Tang, Y.-J. Lee, and T.A. Litzinger, "A Study of the Effects of Pressure Variations on the Deflagration of RDX Composite Propellants," Proceedings of the 32nd JANNAF Combustion Subcommittee Meeting, NASA Marshall Space Flight Center, Huntsville, Alabama, October 23-27, 1995. CPIA Publication 638, Vol. I, pp. 161-171, October, 1995.
- Y.-J. Lee, C.-J. Tang, and T.A. Litzinger, "A Study of Gas-Phase Processes During the Deflagration of RDX Composite Propellants Using a Triple Quadrupole Mass Spectrometer," 31st JANNAF Combustion Subcommittee Meeting, October 17-21, 1994, Sunnyvale, CA, CPIA Public. 620, Vol. II, pp. 425-437.
- Liau, Y.-C., Thynell, S.T., and Yang, V., "Analysis of RDX/GAP Propellant Combustion with Detailed Chemistry," presented at the JANNAF Combustion Subcommittee Meeting, October, 1997.
- Yang, V., and Thynell, S.T., "Recent Advances in Modeling of RDX Propellant Ignition and Combustion," *U.S. Army Workshop on Solid-Propellant Ignition and Combustion Modeling*, M.S. Miller, R.W. Shaw, and D.M. Mann (eds.), Army Research Laboratory ARL-TR-1411, 1997, pp. 34-49.
- Liau, Y.-C., and V. Yang, "On the Existence of Dark-Zone Temperature Plateau in RDX Monopropellant Flame," AIAA-paper 97-0589, presented at the 35th Aerospace Sciences Meeting, Reno, Nevada, January 8-11, 1997; also presented at the 1996 JANNAF Subcommittee Meeting, Naval Postgraduate School, Monterey, CA, November 4-8, 1996.
- Liau, Y.-C., and V. Yang, "An Improved Model of Laser-Induced Ignition of RDX Monopropellant," CPIA Publication 653, Vol. 2, pp. 529-545, 1996; 33rd JANNAF Subcommittee Meeting, Naval Postgraduate School, Monterey, CA, November 4-8, 1996.
- Liau, Y.-C., and V. Yang, "Analysis of RDX Mono-Propellant Combustion with Two-Phase Subsurface Reactions," *Journal of Propulsion and Power*, Vol. 11, No. 4., July-Aug., pp.729-739, 1995.
- Yang, V. and Zarko, V.E. (eds.), *Solid-Propellant Rocket Motor Interior Ballistics and Combustion of Energetic Materials*, published as a special issue of the *Journal of Propulsion and Power*, Vol. 11, July-August 1995.
- Yang, V., and Y.-C. Liau, "A Time-Accurate Analysis of RDX Monopropellant Combustion with Detailed Chemistry," Proceedings of the 32nd JANNAF Combustion Subcommittee Meeting, NASA Marshall Space Flight Center, Huntsville, Alabama, October 23-27, 1995. CPIA Publication 638, Vol. I, pp. 57-67, October, 1995.
- Liau, Y.-C., and V. Yang "Analysis of Nitramine Propellant Combustion with Two-Phase Subsurface Reactions," 31st JANNAF Combustion Subcommittee Meeting, Oct. 17-21, 1994, Sunnyvale, CA.

Brill, T.B., "Surface Pyrolysis Phenomena and Flame Diagnostics by FTIR Spectroscopy," *Non-Intrusive Combustion Diagnostics*, Kuo, K.K., and Parr, T.P. (Eds.), Begell House, Inc., 1994, pp. 191-208.

## **D. LIST OF PARTICIPATING SCIENTIFIC PERSONNEL AND DEGREES RECEIVED**

### **I. Personnel**

Kenneth K. Kuo, Distinguished Professor and Director of the High-Pressure Combustion Laboratory  
Thomas B. Brill, Professor, University of Delaware - Subcontractor  
Paul W. Brown, Professor  
Wen H. Hsieh, Assistant Professor  
Thomas A. Litzinger, Professor  
Stefan T. Thynell, Professor  
Vigor Yang, Professor  
Y.C. Lu, Research Associate  
Y.-C. (John) Liao, Ph.D. Candidate, URI-Fellow  
Carl Mallery, Ph.D. Candidate, URI-Fellow  
Gautam Kudva, Ph.D. Candidate, URI-Fellow  
Abdullah Ulas, Ph.D. Candidate, URI-Fellow  
Eric Boyer, Ph.D. Candidate  
Polly Gongwer, Ph.D. Candidate, University of Delaware - Subcontractor  
J. Wu, URI Post-Doc Fellow  
Barry Fetherolf, Ph.D. Candidate, URI-Fellow  
Peter I. Huang, Ph.D. Candidate  
Sean Wilson, Master's Student, URI-Fellow  
Julian Laxton, M.S. Student  
Todd Freyman, M.S. Student  
Gerardo Hernandez, Summer Student  
Kevin Desmarais, Summer Student  
Y.S. Tseng, Undergraduate Honor Student  
Eun Kim, Undergraduate Student

### **II. Degrees Awarded**

Polly E. Gongwer, Doctor of Philosophy in Chemistry, University of Delaware, May 1998.  
Carl F. Mallery, Doctor of Philosophy in Mechanical Engineering, The Pennsylvania State University, August 1997.  
Y.-C. Liao, Doctor of Philosophy in Mechanical Engineering, The Pennsylvania State University, May 1997.  
E. Boyer, Master of Science in Mechanical Engineering, The Pennsylvania State University, August, 1996.  
A. Ulas, Master of Science in Mechanical Engineering, The Pennsylvania State University, May 1996.

- T. Freyman, Master of Science in Mechanical Engineering, The Pennsylvania State University, August 1995.
- S. Wilson, Master of Science in Materials Science and Engineering, The Pennsylvania State University, August 1995.
- J. Laxton, Honored Undergraduate Student, Bachelor of Science in Mechanical Engineering, The Pennsylvania State University, January, 1995.
- Y.S. Tseng, Honored Undergraduate Student, Bachelor of Science in Aerospace Engineering, The Pennsylvania State University, January, 1995.
- B. Fetherolf, Doctor of Philosophy, Mechanical Engineering, The Pennsylvania State University, January 1994.
- I.T. Huang, Doctor of Philosophy, Mechanical Engineering, The Pennsylvania State University, January 1994.

## **E. INVENTIONS**

None.